Large-scale particulate air pollution and chemical fingerprint of volcanic sulfate aerosols from the 2014–15 Holuhraun flood lava eruption of Bárðarbunga volcano (Iceland).

Marie Boichu[1,2], Olivier Favez[3], Véronique Riffault[4], Colette Brogniez[2], Jean Sciare[5], Isabelle Chiapello[1,2], Lieven Clarisse[6], Shouwen Zhang[4,7], Nathalie Pujol-Söhne[7], Emmanuel Tison[4], Hervé Delbarre[8], and Philippe Goloub[2]

[1]Centre National de la Recherche Scientifique, France
[2]Laboratoire d'Optique Atmosphérique, Université de Lille, CNRS/INSU, UMR8518, Villeneuve d'Ascq, France
[3]Institut National de l'Environnement Industriel et des Risques (INERIS), Verneuil-en-Halatte, France
[4]IMT Lille Douai, SAGE, Douai, France
[5]Laboratoire des Sciences du Climat et de l'Environnement (CNRS-CEA-UVSQ), CEA Orme des Merisiers, Gif-sur-Yvette, France. Now at the Cyprus Institute, Nicosia, Cyprus
[6]Spectroscopie de l'Atmosphère, Service de Chimie Quantique et Photophysique, Université Libre de Bruxelles, Brussels, Belgium
[7]Atmo Hauts de France, Lille, France
[8]Laboratoire de Physico-chimie de l'Atmosphère, Université du Littoral Côte d'Opale, Dunkerque, France

Correspondence: Marie Boichu (marie.boichu@univ-lille.fr)

Abstract. Volcanic sulfate aerosols play a key role on air quality and climate. However, the oxidation of sulfur dioxide (SO_2) precursor gas to sulfate aerosols (SO_4^{2-}) in volcanic clouds is poorly known, especially in the troposphere. Here we determine the chemical speciation, lifetime and impact on air quality of sulfate aerosols from the 2014–15 Holuhraun flood lava eruption of Bárðarbunga icelandic volcano. To do so, we jointly analyze a set of SO_2 observations from satellite (OMPS and

5   IASI) and ground-level measurements from air quality monitoring stations together with, for the first time, high temporal resolution mass spectrometry measurements of Aerosol Chemical Speciation Monitor (ACSM) performed far from the source. We explore month/year-long ACSM data in France from stations in contrasted environments, close and far from industrial sulfur-rich activities. We demonstrate that aged volcanic sulfate aerosols exhibit a distinct chemical fingerprint, with NO_3:SO_4 and Organic:SO_4 concentration ratios higher than freshly-emitted industrial sulfate but lower than background aerosols in urban/rural conditions. Combining AERONET (AErosol RObotic NETwork) sunphotometric data with ACSM observations, we

10   also show a long persistence over weeks of volcanic sulfate aerosols while SO_2 disappears in a few days at most. Finally, gathering 6 month-long datasets from 19 sulfur monitoring stations of the EMEP (European Monitoring and Evaluation Programme) network allows us to demonstrate a much broader large-scale European particulate pollution in SO_4 associated to the Holuhraun eruption, from Scandinavia to France. Exploiting these in-situ data, we also show the various rates of SO_2 oxidation

15   observed in the volcanic cloud, with SO_2:SO_4 concentration ratios ranging in 0.6–7, distinct from background conditions of about 50. Most current studies generally focus on SO_2, an unambiguous and more readily measured marker of the volcanic

cloud. However, our results here on sulfate aerosols raise fundamental questions about the cumulative impact of tropospheric eruptions on air quality, health, atmospheric composition and climate, which may be significantly underestimated.

1 Introduction

Volcanic sulfate aerosols play a key role on climate. While the direct radiative forcing caused by scattering of incoming solar radiation by stratospheric sulfate aerosols from major eruptions is well known (Robock, 2000), the climate effect of sulfate aerosols from smaller eruptions, reaching the lower stratosphere or restricted to the troposphere, has been overlooked and underestimated. Indeed, moderate eruptions, which have a much greater frequency, may be capable of sporadically feeding the stratospheric aerosol load (Vernier et al., 2011; Neely et al., 2013; Ridley et al., 2014). The identification by CMIP5 (Coupled Model Intercomparison Project) of a systematic bias toward underestimation of the cooling of the lower stratosphere and overestimation of the troposphere warming (also called 'warming hiatus') over 1998-2012 in current global circulation models might be partly due to an inappropriate account of these smaller volcanic eruptions (Solomon et al., 2011; Santer et al., 2014). Hence, the impact of tropospheric eruptions on radiative forcing, generally neglected, deserves greater attention. Sulfate aerosols can be rapidly washed out by precipitations in the troposphere, which favors a shorter lifetime relative to stratospheric aerosols. However, sulfate aerosols reduce the nucleation rate of ice crystals, affecting the properties of the ubiquitous upper troposphere cirrus clouds that play a critical role on climate (Kuebbeler et al., 2012). The properties of low-altitude meteorological clouds, their formation, lifetime and precipitation can be also substantially affected by the presence of volcanic sulfate aerosols in the lower troposphere, that are issued from persistent passive degassing activity (Gassó, 2008; Schmidt et al., 2012; Ebmeier et al., 2014) or from effusive eruptions (Yuan et al., 2011; McCoy and Hartmann, 2015; Malavelle et al., 2017).

Volcanic sulfate aerosols in the troposphere, the topic of this paper, also have a detrimental impact on air quality and human health, as they represent a dominant component of fine particulate matter characterized by a diameter less than 2.5 μm. Owing to their small size, these aerosols have slow settling velocities and thus can accumulate in the boundary layer and penetrate deeply into the lung, exacerbating symptoms of asthma and cardiorespiratory diseases (Delmelle, 2003; Thordarson and Self, 2003; Longo et al., 2008; van Manen, 2014). They also adversely affect the environment, with deleterious effects on vegetation, agriculture, soils and groundwater (Delmelle, 2003; van Manen, 2014; Thordarson and Self, 2003; Oppenheimer et al., 2011). Last but not least, sulfate aerosols can damage aircraft engines (Carn et al., 2009), a poorly-known impact especially under repeated aircraft encounters with diluted volcanic clouds as recently tolerated by legislation (ICAO, 2016).

Volcanic sulfate aerosols can be divided in two categories, either of primary or secondary nature. Primary sulfate aerosols are directly emitted at the vent, as observed at a few volcanoes worldwide (e.g. Allen et al. (2002); Mather et al. (2003b, 2004);

Zelenski et al. (2015)). On the other hand, secondary sulfate aerosols result from in-plume oxidation of sulfur dioxide (SO_2), one of the most abundant gas species emitted by volcanoes, during transport downwind (Oppenheimer et al., 2011; Pattantyus et al., 2018). Dominant pathways have been identified for this SO_2-to-sulfate conversion in the troposphere via both gas- and aqueous-phase processes. In the gas phase, SO_2 oxidation predominantly occurs by reaction with hydroxyl radicals (OH) to

5   form sulfuric acid (H_2SO_4) according to the reactions (Seinfeld and Pandis, 2012):

$$SO_{2(g)} + OH + M \longrightarrow HOSO_2 + M$$
$$HOSO_2 + O_2 \longrightarrow HO_2 + SO_3$$
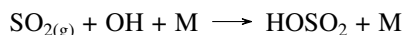
10   where M is another molecule (usually N_2) that is required to absorb excess kinetic energy from the reactants. In presence of water vapour, SO_3 is then rapidly converted to $H_2SO_{4(g)}$:

$$SO_3 + H_2O + M \longrightarrow H_2SO_{4(g)} + M$$
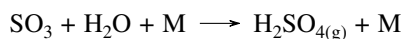
15   Due to its highly hygroscopic nature, $H_2SO_{4(g)}$ is efficiently taken up to the aqueous phase to form sulfate aerosols (Seinfeld and Pandis, 2012) following the reactions:

$$H_2SO_{4(g)} + H_2O \longrightarrow H_3O^+ + HSO_4^-$$
$$HSO_4^- + H_2O \longrightarrow H_3O^+ + SO_4^{2-}$$
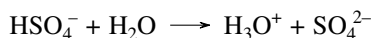
As shown in volcanic clouds, $H_2SO_{4(g)}$ can also nucleate to form new particles (Boulon et al., 2011). Gas-phase SO_2 oxidation takes place on a timescale of weeks in the troposphere.

Much faster oxidation occurs, over hours or days, through heterogeneous reactions in the aqueous phase if SO_2 is taken up to

25   particles, either aerosols or cloud droplets. SO_2 easily dissolves in water and can form three different chemical species depending on pH values: 1- bisulfite ion (HSO_3^-), the preferential sulfur species for pH values in [2–7]; 2- hydrated SO_2 ($SO_2.H_2O$), for low pH values (pH < 2); and 3- sulfite ion (SO_3^-) for basic pH values (pH > 7), according to equilibrium reactions (Seinfeld and Pandis, 2012):

30     $$SO_{2(g)} + H_2O \rightleftharpoons SO_2 \cdot H_2O$$

$$SO_2 \cdot H_2O \rightleftharpoons H^+ + HSO_3^-$$

$$HSO_3^- \rightleftharpoons H^+ + SO_3^{2-}$$
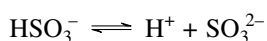
These three species have a sulfur oxidation state equal to 4, referred to as S(IV). Oxidation of these S(IV) species to sulfate aerosols (SO_4^{2-}), whose sulfur oxidation state is equal to 6 (S(VI)), is mainly known to occur by reaction with dissolved ozone (O_3) for pH > 5.5 and with hydrogen peroxide (H_2O_2) as follows (Seinfeld and Pandis, 2012; Stevenson et al., 2003):

5 $$S(IV) + O_3 \longrightarrow S(VI) + O_2$$
$$S(IV) + H_2O_2 \longrightarrow S(VI) + H_2O$$
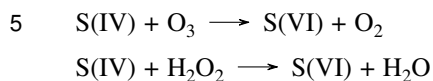
In volcanic plumes, S(IV) can also be oxidized in the aqueous phase by dissolved oxygen (O_2) catalyzed by iron and manganese (Seinfeld and Pandis, 2012) and halogen-rich species (HOBr or HOCl) as shown more recently by von Glasow and
10 Crutzen (2003).

Therefore, SO_2 oxidation to sulfate within volcanic clouds involves complex processes in the gas- and aqueous-phases depending on many variables including solar insolation, relative humidity, temperature, pH of aerosol/cloud droplets and concentrations of the various volcanic gas species and ash particles. As such, the rate of production of volcanic sulfate aerosols
15 is still poorly known, with a large range of rates observed in different volcanic environments in the world, as summarized in Pattantyus et al. (2018).

The chemical speciation of volcanic sulfate aerosols has been poorly studied until now and is also barely known. Some observations have been occasionally collected, using filter packs or cascade impactors, during short fieldtrips near the vent of
20 a few volcanoes worldwide (e.g. (Mather et al., 2003a; Martin et al., 2011; Ilyinskaya et al., 2011). However, such methods only provide an average representation of the chemical composition of aerosols over the duration of instrument exposure to volcanic emissions. In addition to the low temporal resolution of these limited-time observations, a tedious and careful post-collection laboratory analysis is required to avoid biases. To our knowledge, one single study of Kroll et al. (2015) explored through near real-time quasi-continuous measurements the partitioning between SO_2 and sulfate aerosols taking
25 place near-source at the strongly degassing Kilauea volcano in 2013. However, such observations have not been performed to thoroughly investigate the chemical speciation of volcanic sulfate aerosols at a long distance from the source. Nonetheless, various volcanic eruptions or persistent passive degassing activities (e.g. Laki/Iceland in 1783–84, Miyake-jima/Japan in 2001, Erebus/Antarctica, Holuhraun eruption of Bárðarbunga volcano/Iceland in 2014–15) have been shown to trigger, at a large scale, modifications of the atmospheric chemistry and air pollution episodes in SO_2 (Tu et al., 2004; Schmidt et al., 2015;
30 Ialongo et al., 2015; Boichu et al., 2016; Steensen et al., 2016) and sulfate aerosols (Radke, 1982; Thordarson and Self, 2003; Boichu et al., 2019 in prep).

In this paper, we propose to fill this gap by exploring the chemical fingerprint of volcanic sulfate aerosols after long-range transport and by assessing the intensity of air pollution that these particles can generate at a large scale. We benefit here from a recently developed technology based on near real-time mass spectrometry, named Aerosol Chemical Speciation Monitor
35 (ACSM), which provides mass and chemical composition of the non-refractory fraction of submicron particles at high tempo-

ral resolution. By gathering a large set of ground level in-situ as well as space- and ground-based remote sensing observations (Section 2), this study aims first to quantify the intensity of air pollution in sulfur-rich particles caused by the Holuhraun eruption of Bárðarbunga volcano (Iceland) (Sections 3.1 and 3.2). Secondly, we propose to explore whether the chemical fingerprint of volcanic sulfate aerosols is distinct from those of background aerosols in industrial or urban environments (Section 3.3).

5   To achieve these goals, along with satellite SO_2 observations from OMPS/Suomi NPP and IASI/MetOp-A sensors, we exploit ground-level in situ observations of SO_2 from regional air quality monitoring stations and ACSM measurements performed at two French research sites in contrasted environments, near or far from industrial sulfur-rich emitting activities. Both sites were indeed impacted by sulfur dioxide and sulfate aerosols in relation with the Holuhraun eruption of Bárðarbunga volcano (Iceland) on repeated occasions in September 2014. In a third stage, the joint analysis of in situ ACSM measurements with sun-

10   photometry column observations from co-located stations of the AERONET AErosol RObotic NETwork allows to demonstrate the volcanic origin of an increased aerosol abundance persisting over several weeks in September 2014 (Section 3.4). Finally, to provide a broader picture, we explore 6-month long sulfur monitoring datasets (Sept. 2014-Feb. 2015) from 19 stations of the EMEP (European Monitoring and Evaluation Programme) network to evaluate the large-scale impact of the Holuhraun eruption on European aerosols and the range of partitioning of volcanic SO_2 to SO_4 according to the volcanic cloud history

15   (Section 3.5).

2   Observations

2.1   Ground-level in-situ observations

2.1.1   Aerosol chemical speciation monitor

The chemical composition of non-refractory submicron aerosols (NR-PM_1), including sulfate (SO_4^{2-}), nitrate (NO_3^-), am-

20   monium (NH_4^+) and organic (Org) species, are monitored with a time resolution of about 30 min and detection limits of 0.2 μg m^{-3}, using quadrupole Aerosol Chemical Monitors (ACSM) at two French sites with contrasting background conditions (Dunkirk and SIRTA). Note that charges of inorganic species, determined as ions by ACSM, are not systematically indicated in text and figures hereafter, to ease readability.

25   For a detailed description of the ACSM, developed by Aerodyne Research Inc., the reader is referred to Ng et al. (2011). Briefly, aerosols are sampled into the instrument through a critical orifice mounted at the inlet of a PM_1 aerodynamic lens and focused under vacuum to an oven at the temperature of 600°C. Flash vaporized molecules are then ionized at 70eV electron impact before being detected and quantified by the mass spectrometer. Raw data are corrected for aerosol collection efficiency following the protocol defined by Middlebrook et al. (2012). A specific ionization efficiency (relative to nitrate, RIE) should

30   also be defined for each species. For the Dunkirk ACSM, a constant 0.55 SO_4 RIE has been used, based on results obtained from calibrations performed regularly (typically, every 2 months) during the campaign. By the time of the measurement, a default SO_4 RIE value was preferably taken as equal to 1.20 for the SIRTA ACSM (Ng et al., 2011; Crenn et al., 2015). There-

fore, most figures hereafter display ACSM data processed using these values of 0.55 and 1.20 for the Dunkirk and SIRTA datasets, respectively. However, it may be noted that recent optimizations of the ACSM calibration procedure are currently allowing to assess SO_4 RIE values more accurately (Xu et al., 2018; Freney et al., subm). In particular, a value of 0.86 was obtained in spring 2016 when applying the new calibration procedure for the first time to the ACSM at SIRTA (Freney et al., subm). Impacts of the choice of the RIE value on SO_4 concentrations used in the present study are evaluated in Section 3.3.3. Such differences are still in the range of uncertainties (15-36%) estimated for the measurements of major submicron chemical species using ACSM (Budisulistiorini et al., 2014; Crenn et al., 2015).

Dunkirk located in northern France (latitude 51.052°N, longitude 2.348°E, map in inset of Fig. 1) hosts a large harbour, ranking 7th in Europe, with a developed manufacturing industry (map in Fig. A1) accounting for more than 80% of total particulate matter (PM) emitted locally over 2009-2011 (Clerc et al., 2012). About 97% of primary PM_1 are emitted by metallurgy, steel and smelter activities (Fig. 1-7 of Zhang (2016)). A remarkable 14 month-long 30 min-resolved ACSM dataset has been collected at Port-East site (map in Fig. A1), with collocated ground-level SO_2 measurements, from 15 July 2013 to 11 Sept 2014 (Zhang, 2016), allowing us to compare the chemical fingerprint of industrial and volcanic sulfate aerosols.

The SIRTA facility (Site Instrumental de Recherche par Télédétection Atmosphérique, http://sirta.ipsl.fr, Haeffelin et al. (2005), latitude 48.713°N and longitude 2.214°E), is located about 20 km southwest of the Paris city center (map in inset of Fig. 2). This atmospheric observatory is notably part of the European Aerosol, Clouds and Traces gases Research InfraStructure (ACTRIS, www.actris.eu) as a peri-urban station for remote sensing and in-situ measurements representative of background PM levels of the Paris region. ACSM data have been routinely collected there since the end of 2011 (Petit et al., 2015). A 2-month hourly-resolved dataset (Sept-Oct 2014) has been used for the purpose of the present study to investigate the speciation of volcanic sulfate aerosols, especially during the largest event of volcanogenic air pollution affecting France in late September 2014 (Boichu et al., 2016).

2.1.2 SO_2 mass concentrations from French air quality monitoring network

Ground-level mass concentrations of SO_2 are routinely monitored using ultraviolet fluorescence analyzers by regional air quality monitoring networks, with a detection limit of 5.3 μg m^{-3} and an uncertainty never exceeding 15%. For the present study, data from Atmo Hauts-de-France and Airparif could be explored, corresponding to the following stations: Dunkirk (Port East site), Calais-Berthelot, and Malo-les-Bains on the one hand, and Neuilly-sur-Seine and Vitry-sur-Seine on the other hand (maps in inset of Figures 1 and 2). Hourly mean data have been used here for all stations but the Port-East one in Dunkirk with 15-min time resolution.

2.1.3 Filter pack measurements from the EMEP network

The EMEP (European Monitoring and Evaluation Programme, http://ebas.nilu.no) network, in charge of monitoring air pollution and surface deposition with harmonized measurements across Europe, gathers ground stations that are weakly affected

by local sources of pollution (Tørseth et al., 2012). We focus here on stations where filter pack measurements provide daily ground-level mass concentrations of both gaseous SO_2 and particulate SO_4 (PM_{10} fraction). Unfortunately, at the time of the Bárðarbunga Holuhraun eruption in 2014–15, such measurements were not performed anymore in many North-Western European countries including France, Belgium, the Netherlands and the United Kingdom. The network still adequately covers

5 Scandinavia (Finland, Sweden, Norway and Denmark) and only a few remaining stations are left in Germany and Ireland. We consequently explore in this study data from 19 stations based in Finland, Norway, Sweden, Denmark, Germany, Ireland and Russia.

2.2 Satellite observations of the volcanic SO_2 cloud

Ultraviolet (UV) observations from OMPS (Ozone Mapping and Profiler Suite)/SNPP (Suomi National Polar-orbiting Partner-

10 ship) sensor, with pixel size at nadir of 50 km × 50 km and Equator crossing time of 13:30 local time (Carn et al., 2015), allow tracking the large-scale dispersal of the Bárðarbunga SO_2-rich cloud and identifying the dates it is transported over specific ground stations. According to IASI satellite observations described below, the altitude of Bárðarbunga SO_2 is most often lower than 6 km over France (see the Animation of IASI observations of the Holuhraun SO_2 cloud dispersal in Supplementary Material). Consequently, the Level-2 planetary boundary layer (PBL) products for the SO_2 total column are chosen to study the

15 dispersal of the Holuhraun cloud over France.

Infrared Atmospheric Sounding Interferometer (IASI) observations from polar-orbiting MetOp-A satellite, with a pixel footprint at nadir of 12 km diameter, full swath width of 2200 km and Equator crossing time at 9:30 and 21:30 local time. IASI observations are generally less sensitive than OMPS to SO_2 below 5 km of altitude (Boichu et al., 2016). However,

20 IASI benefits from a shorter revisit interval (i.e. 12 hours) and provides both column amount and altitude of SO_2. After the retrieval of the SO_2 altitude using the algorithm described in detail in Clarisse et al. (2014), an optimal estimation scheme with generalized noise covariance is used for SO_2 column retrieval (Bauduin et al., 2014).

2.3 Column-integrated aerosol properties from the AERONET ground-based remote sensing network

Time series of daily averaged Aerosol Optical Depth (AOD) at 500 nm, derived from Direct Sun photometer measurements

25 (Version 3, Level 2.0, in cloud-free conditions) from the AErosol RObotic NETwork (AERONET) (Holben et al., 2001), are exploited at the two French sites of Dunkirk (map in Fig. A1 of the precise location of the station on Dunkirk Port) and SIRTA.

3 Results and discussion

First, we evaluate the intensity of air pollution in sulfur-rich particles induced by the Bárðarbunga eruption in France. We also propose to explore whether the fingerprint of sulfate aerosols is specific or not within volcanic clouds, by comparison with

30 sulfate aerosols of industrial origin. We then define a methodology to discriminate volcanic versus regional industrial sulfur-rich compounds. To do so, we study several volcanogenic events of air pollution observed in France in September 2014 at two

locations nearby (Dunkirk) and distant (SIRTA) from industrial activities. Then, we investigate whether air pollution events, that are characterized by anomalies in ground-level SO_2 and SO_4 mass concentrations, are also detected more broadly, at the European scale, by exploiting data from the EMEP ground network. Finally, we examine whether the distinct SO_2 vs. SO_4 signature of sulfate aerosols of volcanic origin highlighted in France is observed at other EMEP stations in Europe.

3.1 Volcanogenic short-term events of air pollution

SO_2 is commonly used as a marker of volcanic plumes. Hence, OMPS satellite SO_2 observations allow to detect when the volcanic cloud passes over the two French sites equipped with ACSM (i.e. Dunkirk and SIRTA), bearing in mind that satellite ultraviolet observations of SO_2, aside from their detection limit, have a lower sensitivity especially in the lower troposphere and the planetary boundary layer (Krotkov et al., 2008). Top of Fig. 1 indicates that a branch of the Bárðarbunga SO_2 cloud passes over Dunkirk in northern France on 7 Sept 2014 and air masses containing volcanic SO_2 are still detected over Dunkirk on 10 Sept 2014. Concomitantly, high peak values in ground-level SO_4 mass concentration up to ≈ 10 μg m^{-3} (middle of Fig. 1) are recorded by 30 min-resolved ACSM measurements at Dunkirk and large anomalies in SO_2 concentration (up to 70 μg m^{-3}) are regionally measured by various air quality stations of Nord-Pas de Calais, as exemplified here at Dunkirk Port-East with 15 min-resolved measurements (middle of Fig. 1), and hourly observations at Malo-les-Bains and Calais Berthelot (bottom of Fig. 1).

It should be pointed out that high peaks in both ground-level SO_2 (up to ≈ 80 μg m^{-3}) and SO_4 (up to ≈ 9 μg m^{-3}) concentrations, are also recorded at Dunkirk Port-East on 1 Sept 2014 before the arrival of the Bárðarbunga cloud over France. In contrast to other days in early Sept 2014 of intense air pollution in SO_2, the meteorological station at Port-East also indicates that on 1 Sept 2014 local winds originate from the nearby industrial site before passing over Port-East station with a wind direction of about 270° (Fig. A2). Hence, the ground-level concentration in volcanic sulfate aerosols on 7 Sept 2014, despite a transport and dispersion of emissions over a few thousands of kilometers from Iceland to France, is of similar magnitude to the concentration in sulfate aerosols emitted on 1 Sept by a nearby industrial site hosting metallurgy activities.

To conclude, this set of simultaneous observations, from the ground at a regional scale and from space, allows to demonstrate the volcanogenic origin of the two peak values in ground-level SO_4 concentration recorded in Dunkirk on 7 Sept between 07:36 and 23:19 UTC (hereafter named "DK volcanic event 1") and the second between 10 Sept 20:00 and 11 Sept 2014 05:50 UTC (hereafter named "DK volcanic event 2") (Fig. 1).

Similarly, exploiting OMPS satellite maps and Airparif SO_2 measurements at various air quality monitoring stations of the Paris region (only Vitry-sur-Seine and Neuilly-sur-Seine are shown here) demonstrates the volcanic origin of the largest event of air pollution in sulfate aerosols (with a ground-level concentration up to 16 μg m^{-3}), in terms of magnitude and duration, recorded with ACSM at SIRTA between 21 and 25 Sept 2014 (hereafter named "SI volcanic event") (Fig. 2). This particulate pollution is concomitant with a pronounced air pollution in SO_2, with a ground-level concentration up to 80 μg m^{-3} in the Paris region (bottom of Fig. 2) but also more broadly at various places in Northern France as observed by Boichu et al. (2016). Nevertheless, despite these high SO_2 concentrations measured regionally at ground-level on that day (Bottom of Fig. 2), it is interesting to point out that, on 24 Sept, neither OMPS nor OMI satellite observations are sensitive enough to detect any SO_2

over the northern part of France encompassing the Paris region (OMI satellite data not shown here). This demonstrates the necessity to combine both space and ground observations, especially when SO_2 is confined in the boundary layer. Note that the two simultaneous anomalies observed on 9 and 10 Sept 2014 in both SO_4 at SIRTA and SO_2 concentrations at Airparif stations may also be volcanogenic. Nevertheless, this 2-day long episode of air pollution is not selected for further analysis as

5   it is of lower intensity compared to the three other volcanogenic events already selected.

3.2   Background air pollution in sulfur-rich gas and aerosol species

At SIRTA, a 2-month average SO_4 mass concentration of 1.00 μg m^{-3} is recorded with hourly-resolved ACSM data during the Sept-Oct 2014 period while the concentration rises up to 16 μg m^{-3} between 21 and 25 Sept 2014 during the largest event of

10   volcanogenic pollution in SO_2 recorded in France (Fig. 2). Over the same period of time, air quality monitoring stations of the region record a mean mass concentration in SO_2 of 1.4 and 1.9 μg m^{-3} at Neuilly-sur-Seine and Vitry-sur-Seine respectively, which peaks at 80 and 42 μg m^{-3} during the volcanogenic pollution episode in late September 2014. Note that two other high peaks in SO_2 concentration (up to about 70 and 50 μg m^{-3}) are also observed in early October 2014, coincident with low SO_4 concentration values. These anomalies are not of volcanic origin according to OMPS and IASI SO_2 observations (see

15   Animations of OMPS and IASI observations of the Holuhraun cloud dispersal in Supplementary Material). They are clearly associated to local emissions, since they are not recorded simultaneously at the three air quality stations of the Paris region, and may be linked to heating systems turned on again before winter.

By comparison, Dunkirk Port East is a much more polluted site in sulfur compounds as revealed by mean concentrations in SO_4 of 2.35 μg m^{-3} and in SO_2 of 10.4 μg m^{-3} over a 14 month period (15 Jul 2013–11 Sept 2014) (top of Fig. 3), which

20   represent concentrations in SO_4 and SO_2 respectively more than twice and five times larger than at SIRTA.

3.3   Chemical fingerprint of volcanic sulfate aerosols

3.3.1   Chemical fingerprint of volcanic and background aerosols at two contrasting sites

The 14-month long ACSM dataset with a resolution of 30 min collected between 15 Jul 2013 and 11 Sept 2014 in Dunkirk

25   indicates large fluctuations, up to 40 μg m^{-3}, in the concentration of sulfate aerosols at ground-level (top of Fig. 3). Large variations in ground-level SO_2 concentrations, up to 340 μg m^{-3}, are also recorded by Atmo Hauts-de-France air quality stations. However, no constant correlation is observed between SO_2 and SO_4 mass concentrations over the Jul 2013–Sept 2014 period of interest (top of Fig. 3). Significant fluctuations in concentrations are also shown for NO_3 (variations up to 30 μg m^{-3}), NH_4 (up to 20 μg m^{-3}) and organic aerosols, the latter presenting the most important variations (up to 70 μg m^{-3}) (middle of

30   Fig. 3).

Although investigated here on a shorter period of 2 months (Sept-Oct 2014), variations in submicron particle concentrations at the SIRTA platform are much more limited with peak values of 16, 13, 11 and 4 μg m^{-3} for SO_4, organic, NO_3 and NH_4

aerosols respectively (Fig. 4). At SIRTA, unlike nitrate and organics, the highest concentrations in ammonium aerosols are recorded between 21 and 25 Sept 2014, a period corresponding to the largest volcanogenic event of air pollution in sulfur-rich gas and particulate species in France (Section 3.1).

5   Scatter plots of the concentrations of gaseous SO_2, measured by air quality stations, and of the various aerosol species (NH_4, NO_3, Org) measured with ACSM, versus the concentration of sulfate aerosols, at the two sites of SIRTA (in black) and Dunkirk (in grey), display a wide dispersion of data (top of Figures 5 and 6). As described previously in Section 3.1, three episodes of volcanogenic air pollution in SO_2 have been highlighted at Dunkirk and SIRTA in Sept 2014. The ACSM data collected during the time period of occurrence of these volcanic events are marked specifically in the bottom of Figures 5 and 6 (red squares

10   for the largest event of air pollution in volcanic SO_2 and SO_4 that is recorded at SIRTA, green triangles and circles for DK volcanic events 1 and 2, respectively).

    As Dunkirk is a much more polluted site than SIRTA, with various types and sources of aerosols, we start by comparing the signature of volcanic aerosols to SIRTA background. We observe that volcanic aerosols at both sites can be clearly distinguished

15   from SIRTA (SI) background aerosols (in blue), especially in the scatter plots of SO_2 (bottom of Fig. 5-A), NO_3 (bottom of Fig. 6-C) and Org (bottom of Fig. 6-D) *vs.* SO_4 mass concentrations.

    Focusing on the NO_3 *vs.* SO_4 scatter plot (bottom of Fig. 6-C), we observe that the concentrations of SO_4 in SI background values are much lower (≤ 4 μg m^{-3}) than during volcanic events at both sites (rising up to 16 μg m^{-3}). A wider range of NO_3 concentrations is also recorded during volcanic events, with a maximum of ≈ 15 μg m^{-3} during DK volcanic event 1

20   and lower values (< 3 μg m^{-3}) during the largest volcanic event while background concentrations at SIRTA never exceed ≈ 11 μg m^{-3}. Globally, we observe that volcanic aerosols at both sites display a lower NO_3:SO_4 concentration ratio than background aerosols at SIRTA, thus exhibiting a clearly distinct pattern.

    In contrast to NO_3, a narrower range of organics concentrations is observed during volcanic events (< 9 μg m^{-3}) than during background conditions at SIRTA with Org concentrations up to 13 μg m^{-3} (bottom of Fig. 6-D). Again, volcanic

25   aerosols present a distinct behavior with a much lower Org:SO_4 mass concentration ratio compared to SI background aerosols. Similarly, volcanic aerosols display a much lower SO_2:SO_4 concentration ratio than background aerosols (bottom of Fig. 5-A).

    However, isolating volcanic aerosols from SI background is less obvious in the scatter plot of NH_4 *versus* SO_4 concentrations. This will be further analyzed next in the text. Whereas higher NH_4 concentrations up to 7 μg m^{-3} are recorded within the volcanic cloud, concentrations are about twice lower in SI background conditions. Hence, volcanic aerosols do not present

30   a NH_4:SO_4 concentration ratio significantly different from SI background characteristics (bottom of Fig. 5-B).

3.3.2   Specific signature of freshly-emitted industrial sulfate-rich aerosols

Concentrations at Dunkirk display a more complex behavior with widely scattered values compared to SIRTA.

We are especially intrigued by a group of ACSM data at Dunkirk that are associated to very low concentrations of NO_3, hence presenting a signature close to the one of the largest volcanic event recorded at SIRTA (red squares) but showing a larger spread of SO_4 concentration values up to 30 μg m^{-3} (bottom of Fig. 6-C). For this reason, we color in cyan these specific data associated to concentrations of NO_3 <1 and SO_4 > 4 μg m^{-3} in the various scatter plots of Figures 5 and 6. We demonstrate in the following that these cyan data points are in fact associated to acid aerosols. To do so, we compare the predicted con-

5   centration of NH_4 with the measured concentration of NH_4 (Fig. 7). According to Seinfeld and Pandis (2012), the preferred form of sulfate in an ammonia - nitric acid - sulfuric acid - water system rich in ammonia and presenting a relatively elevated relative humidity is the neutral $(NH_4)_2SO_4$ form. Under these assumptions, $NH_4, pred$, the predicted concentration of NH_4, is calculated assuming that NH_4^+ has completely neutralized available sulfate, nitrate and chloride ions to form $(NH_4)_2SO_4$, NH_4NO_3 and NH_4Cl aerosols, which writes:

10   $$[NH_{4,pred}] = M_{NH_4} \times \left(\frac{[SO_4]}{M_{SO_4}} \times 2 + \frac{[NO_3]}{M_{NO_3}} + \frac{[Cl]}{M_{Cl}} \right), \tag{1}$$

with molar masses of each species, M_{NH4}, M_{SO4}, M_{NO3} and M_{Cl}, respectively equal to 18, 96, 62 and 35.5 g.mol^{-1}. As the measured concentration of Cl is negligible compared to other species at both sites of Dunkirk and SIRTA according to ACSM observations (data not shown here), the last term in Eq. 1 is neglected.

ACSM data associated to volcanic events and to background conditions in Dunkirk are roughly aligned in the scatter plot of

15   measured versus predicted concentrations of NH_4 along the first bisector (Fig. 7). However, data colored in cyan are widely scattered below the first bisector. This result demonstrates that NH_4^+ ions have not had enough time to neutralize surrounding sulfate and nitrate ions. Consequently, these specific aerosols are acidic, rich in sulfate, relatively poor in ammonium and very poor in nitrate and organic aerosols compared to background aerosols (bottom of Figures 5 and 6). Aerosols with such characteristics are not observed at SIRTA, situated far from an any industrial activities. Therefore, we conclude that these acidic

20   aerosols at Dunkirk represent freshly-emitted aerosols of industrial origin, likely emitted by metallurgy and steel activities.

3.3.3   Best strategy to isolate volcanic sulfate from other types of aerosols

We have shown in Sections 3.3.1 and 3.3.2 that exploring the detailed chemical speciation of aerosols provided by ACSM measurements allows us to isolate the fingerprint of aged volcanic sulfate aerosols (e.g. aerosols already transported over a long distance from their source) from those of freshly-emitted industrial sulfate or background aerosols in various urban, marine or

25   agricultural-influenced environments. As summarized in Fig. 8, angular sectors, which are indicative of the various sources of aerosols according to their color (volcanic in red, freshly-emitted industrial in cyan or background in blue), are more distinctively separated in the scatter plots of NO_3 or Org vs SO_4 mass concentrations, which are thus more informative to identify the aerosol source.

30   To combine in a single plot the information on both the chemical fingerprint of aerosols from these scatter plots as well as their degree of acidity, we represent the variations of the NO_3:SO_4 (top of Fig. 9) or Org:SO_4 (bottom of Fig. 9) mass

concentration ratios versus the ratio of measured to predicted NH_4 concentrations. To avoid a noisy representation, we select ACSM values meeting the criteria $\sqrt{[SO_4]^2 + [NO_3]^2} > 6 \ \mu g \ m^{-3}$ for the top of Fig. 9 and $\sqrt{[SO_4]^2 + [Org]^2} > 6 \ \mu g \ m^{-3}$ for the bottom of Fig. 9.

All aerosols present values of the $NH_4, meas$:$NH_4, pred$ mass concentration ratio close to 1 in agreement with their neu-
5 tralisation, except freshly-emitted industrial aerosols in Dunkirk (in cyan) with most values < 0.75 indicative of their strong acidity (left of Fig. 9).

Nevertheless, we note a few $NH_4, meas$:$NH_4, pred$ values exceeding 1 (up to 1.5) for both the largest volcanic event at SIRTA (in red) and some background aerosols in Dunkirk (in blue) (left of Fig. 9). This phenomenon could be linked with NH_3 uptake onto particulate organic acids, as previously observed in northwestern Europe (Schlag et al., 2017). It may also partly
10 result from possible bias in SO_4 relative ionization efficiency (RIE), as explained in Section 2.1.1. Indeed, the chosen RIE values could lead to an underestimation of SO_4 concentrations and subsequently $NH_4, pred$ values if indeed the true SO_4 RIE was lower. Considering that a SO_4 RIE value of 0.86 was obtained from the new calibration procedure applied for the first time to SIRTA ACSM in spring 2016 (Freney et al., subm), we recalculated SO_4 concentrations using RIE values lower than the chosen one by 28% (i.e., 0.39 and 0.86 for Dunkirk and SIRTA ACSMs, respectively) to investigate the influence of this possible bias.
15 While NO_3:SO_4 and Org:SO_4 mass concentration ratios are weakly influenced by such a change (Fig. 9), it impacts aerosol acidity (Fig. 7 and 9). Indeed, values of the $NH_4, meas$:$NH_4, pred$ mass concentration ratio are lower with a RIE equal to 0.86, independently of the type of aerosols, and do not greatly exceed anymore the value of 1 reducing the bias above mentioned. While volcanic SO_4 aerosols could be overall considered neutralized with a RIE = 1.20 (left of Fig. 7), we note the presence of acidic volcanic aerosols with a RIE = 0.86 (right of Fig. 7), industrial aerosols remaining nevertheless always more acidic than
20 volcanic sulfates. We find that the three periods which are affected by the presence of acidic volcanic aerosols characterized by values of the $NH_4, meas$:$NH_4, pred$ ratio < 0.7 (22 Sept 2014 from 12:00 to 21:00, 23 Sept from 11:00 to 16:00 and 24 Sept from 10:00 to 17:00) are associated to periods of elevated concentrations of SO_4 exceeding 5 $\mu g \ m^{-3}$ (Fig. 2). Note that the most acidic volcanic aerosols, characterized by a weak $NH_4, meas$:$NH_4, pred$ ratio of about 0.5, are recorded on 24 Sept and are associated to SO_4 concentrations > 15 $\mu g \ m^{-3}$. This result suggests that, despite a very long transport over thousands of
25 kilometers from Iceland, the Holuhraun cloud can be sometimes so rich in sulfur that the available amount of ammonia along its way is not sufficient to neutralize all volcanic sulfate aerosols. Indeed, we can also measure at this date the most substantial amounts of volcanic SO_4 at ground-level at SIRTA, with concentrations largely exceeding those of SO_2, a relatively exceptional behavior (Fig. 2). OMPS SO_2 maps (see Animation of OMPS observations of the Holuhraun cloud dispersal in Supplementary Material) indicate that the queue of the Holuhraun cloud arrives over Northern France on 22 Sept and do not seem to greatly
30 move in the following days where it gets diluted according to the observed decrease of SO_2 column amounts with time. Given the simultaneous increase in ground-level concentrations of sulfur-rich species (Fig. 2), this suggests that the volcanic cloud is captured within the planetary boundary layer, hence being more unlikely detected by OMPS. We can wonder whether these specific transport and meteorological conditions favor a larger conversion of SO_2 to SO_4. Notwithstanding, this capture of the Holuhraun cloud within the boundary layer, preventing any more displacement, may explain the lack of local NH_3 to fully neu-

35   tralize volcanic sulfur-rich aerosols, which justifies the presence of remaining acidic H$_2$SO$_4$ aerosols within the volcanic cloud.

Concerning the NO$_3$:SO$_4$ mass concentration ratio, whichever the sulfate RIE coefficient, volcanic aerosols (in red and green) present values between 0.1 and 3, while background aerosols at SIRTA (in blue) are associated to the highest values (> 3) and freshly-emitted industrial aerosols in Dunkirk (in cyan) the lowest values (< 0.15) (top of Fig. 9).

Concerning the Org:SO$_4$ mass concentration ratio, whereas volcanic aerosols present much lower values (mostly < 1.6) compared to background aerosols at SIRTA (> 2.5), industrial aerosols in Dunkirk, even if mostly associated to very low values (< 0.15), can present values similar to volcanic ones up to 1.5. Such a decrease in the concentration of organic aerosols may suggest the formation of organosulfate particles in volcanic aerosols, species that cannot unfortunately be measured by ACSM.

10   This finding would deserve to be further investigated as the hygroscopic properties of organosulfates make them efficient cloud condensation nuclei (Schill and Tolbert, 2013), and as such important climate forcing agents.

Therefore, both NO$_3$:SO$_4$ and Org:SO$_4$ mass concentration ratios allow to distinguish at SIRTA volcanic aerosols from background aerosols. However, the NO$_3$:SO$_4$ ratio seems the most powerful to also isolate the chemical pattern of volcanic aerosols from those of freshly-emitted industrial aerosols as shown in Dunkirk.

Nonetheless, Fig. 9 (as well as Figures 5, 6 and 8) illustrates much more data scatter for background aerosols in Dunkirk (in yellow) compared to SIRTA (in blue), independently of the ratio of interest (NO$_3$:SO$_4$ or Org:SO$_4$). It has to be recalled that the Dunkirk dataset covers a much longer time period (more than a year) than the SIRTA one (2 months), which may partly explain this observation. In addition to its coastal location implying the presence of sulfur-rich aerosols, from marine or ship

20   emissions (Zhang, 2016), that are absent at SIRTA, Dunkirk hosts both intense harbor and industrial activities as previously mentioned (Section 3.2). Therefore, Dunkirk is a much more polluted site in sulfur-rich particles than SIRTA. This certainly explains the significantly broader range of both NO$_3$:SO$_4$ and Org:SO$_4$ ratios observed for Dunkirk background aerosols, with values much lower than for SIRTA background aerosols that even intersect those associated to volcanic aerosols (in red and green). Hence, such a result demonstrates the most challenging issue to discriminate the signature of volcanic aerosols among

25   other types of aerosols at a heavily polluted site.

3.3.4 Thermodynamics of volcanic sulfate aerosols

Fig. 10 shows the scatter plots of NH$_4$ versus NO$_3$ mass concentrations. We find a clear increase in the NH$_4$:NO$_3$ mass concentration ratio for the Holuhraun sulfate aerosols compared to background aerosols. Fig. 6-C and top of Fig. 9 illustrate a

30   pronounced depletion in NO$_3$ within volcanic aerosols while NH$_4$ concentration appears stable or little decreasing (Fig. 5-B). In an ammonia (NH$_3$) – nitric acid (HNO$_3$) – sulfuric acid (H$_2$SO$_4$) – water system, an increase in total sulfate can actually produce a large decrease in NO$_3$ concentration and a significant increase in SO$_4$ concentration but only a slight increase in NH$_4$, as modeled by Seinfeld and Pandis (2012). In an atmosphere very rich in sulfate (e.g. a total sulfate exceeding 25 μg m^{-3}), the

preferred form of sulfate aerosols is not anymore SO_4^{2-} but bisulfate (HSO_4^-). While this thermodynamic model simulation of aerosol composition has been performed for specific atmospheric conditions (temperature of 298 K, relative humidity of 70% and assumptions of an ammonia-rich atmosphere with total ammonia of 10 μg m^{-3} and total nitrate of 20 μg m^{-3}) which may no be exactly those met in Dunkirk and SIRTA in September 2014, model outputs of Seinfeld and Pandis (2012) suggests that the distinct chemical fingerprint observed for Holuhraun aerosols compared to background aerosols, may result from the large

5   abundance of sulfate within the volcanic cloud. Such a high abundance may nevertheless strongly vary far from the volcano according to the volcanic event of interest (Figures 5 and 6), reflecting both various intensities of volcanic source emissions and complex atmospheric histories, which explains the wide range observed in the respective abundance of NO$_3$, NH$_4$, Org and SO$_2$.

3.4 Persistent weeks-long air pollution by volcanic sulfate aerosols

10   We find from ACSM observations some strikingly elevated ground-level concentrations of sulfate aerosols, well in excess to mean values, in September 2014 at both French sites: at SIRTA, over a period of about 2 weeks from 4 to 18 Sept with [SO$_4$]> 0.5 μg m^{-3} (bottom of Fig. 2), and at Dunkirk, over at least 8 days from 3 to 11 Sept with [SO$_4$] > 2 μg m^{-3} (middle of Fig. 1). As shown in Section 3.1, these periods of time are punctuated by a few episodes of volcanogenic pollution in SO$_2$ from Holuhraun eruption: two events at Dunkirk on 7 and 10-11 Sept and two events at SIRTA, a major one on 21-25 Sept

15   but also a more minor episode on 9-10 Sept. Interestingly, these episodes of volcanogenic air pollution in SO$_2$ are short-lived, lasting less than a day or a few days at the most. We consequently wonder whether this persistent particulate pollution in SO$_4$, that is broadly observed in France at locations a few hundreds of kilometers apart, could also be of volcanic origin.

To make progress on this issue, we jointly explore ACSM ground-level in situ measurements with sunphotometer observa-
20   tions from the AERONET (AErosol RObotic NETwork) ground-based remote sensing network (Holben et al., 2001) at the two stations of Dunkirk and SIRTA (Fig. 11). On the period of the persisting anomaly in ground-level SO$_4$ concentration, we also observe elevated values of the aerosol optical depth at 500 nm, > 0.2 at SIRTA (given a mean AOD value of 0.131± 0.035 for September months between the start of AERONET measurements at SIRTA in 2008 and 2016, excluding 2014) and > 0.3 in Dunkirk (given a mean AOD value of 0.175 ± 0.047 for September months between the start of AERONET measurements in

25   Dunkirk in 2006 and 2017, excluding 2014). Most importantly, we find a remarkable correlation between time series of SO$_4$ ground-level mass concentration and of aerosol optical depth at SIRTA (top of Fig. 11) and also at Dunkirk though to a lesser extent due to shorter ACSM dataset (bottom of Fig. 11). This result demonstrates that the aerosol optical depth, a column-integrated property, is mainly controlled by ground-level sulfate aerosols in these occasions. As observed on 1 Sept at Dunkirk (Section 3.1), industrial activities can only trigger short-term peaks, lasting a few hours, in both SO$_2$ and SO$_4$ ground-level

30   mass concentrations (Fig. 1). Therefore, we suggest that the persisting excess anomaly in both SO$_4$ ground-level concentration and aerosol optical depth observed in September 2014 at a regional scale in France may result from the broad dispersion of volcanic sulfur-rich emissions from the Holuhraun eruption.

This result illustrates the much longer lifetime (a few weeks) of volcanic sulfate aerosols compared to SO_2 (a few days), even in the boundary layer. Meteorological conditions, without abundant long-lasting precipitations, have likely favored this persistence of aerosols in the atmosphere. Hence, the impact of the Holuhraun eruption on European air quality, mainly studied through SO_2 observations and atmospheric modelling (Schmidt et al., 2015; Ialongo et al., 2015; Boichu et al., 2016; Steensen et al., 2016) since SO_2 represents a clear marker of volcanic emissions, could have been largely underestimated. This shows that a synergistic analysis of both SO_2 and SO_4 gas/particulate species, combining multi-instrumental and multi-parametric approaches, as developed in this paper, is fundamental to rigorously assess the large-scale impact of volcanic sulfur-rich emissions on atmospheric composition, air quality and health. Holuhraun sulfate aerosols have been shown to strongly affect the microphysical properties of low-altitude meteorological clouds above oceans (McCoy and Hartmann, 2015; Malavelle et al., 2017). This study demonstrates the need to extend such studies above continents to robustly estimate the global volcanic forcing on climate of tropospheric eruptions and persistent passive degassing activities.

3.5 Large scale gas and particulate pollution in sulfur recorded by the EMEP network

To put into perspective our results showing a persistent atmospheric pollution in sulfate particles in France and assess more broadly the geographical impact of Holuhraun emissions on air quality, we explore daily datasets of sulfur monitoring by filter pack measurements from ground stations of the European EMEP network (blue triangles in Fig. 12) over the complete 6-month long eruption (Sep 2014-Feb 2015). We also examine the speciation of volcanic sulfur species (e.g. the SO_2:SO_4 mass concentration ratio here) to see if the speciation observed with ACSM and SO_2 measurements in France is similarly found elsewhere.

Unfortunately, the number of EMEP stations performing sulfur monitoring in Europe has significantly decreased in the last decade. Among the 19 EMEP stations of interest over Europe, we only investigate those presenting a few daily SO_2 concentrations > 3 μg m^{-3} over the Sept 2014–Feb 2015 period, a threshold well above noise level. The six selected stations of interest are located in Scandinavia, their name appear in bold below blue triangles in Fig. 12: Pallas-Matorova FI0036R (Finland), Tustervatn NO0015R (Norway), Bredkälen SE0005R (Sweden), Risoe DK0012R, Anholt DK0008R and Tange DK0003R (Denmark). Note that if a station meets this criterion, the complete SO_2 and SO_4 ground-level mass concentration time series are displayed even if some daily SO_2 mass concentrations are below 3 μg m^{-3} (Fig. 13).

Persistent week-long elevated values in ground-level daily SO_2 mass concentrations (up to > 20 μg m^{-3}), much in excess of background values, are recorded especially in Sept 2014 in Finland (Pallas), Sweden (Bredkälen) and Norway (Tustervatn) to a lesser extent as anomalies are shorter (Fig. 13). During these periods of elevated values in surface SO_2 mass concentrations, increased levels in sulfate mass concentrations are always simultaneously recorded (up to 5 μg m^{-3}). In addition to widespread anomalies in ground-level sulfur concentration suggesting the impact of long-range transported pollutants, the volcanic origin of this atmospheric pollution in sulfur is attested by OMPS and IASI SO_2 observations (see Animations of OMPS and IASI SO_2 observations of the Holuhraun SO_2 cloud in Supplementary Material) showing the Holuhraun volcanic cloud, rich in SO_2, transported repeatedly over Scandinavia in September and early October 2014. Note that Pallas-Matorova, Bredkälen and

Tustervatn represent rural background stations with no significant local or regional air pollution sources, Pallas and Bredkälen being surrounded by coniferous forest or grasslands (Hatakka et al., 2003; Targino et al., 2013) while Tustervatn lies in an agricultural environment poor in sulfur (Aas et al., 2013). EMEP stations in Denmark are less impacted by volcanic emissions. By comparison, they lie in a much more polluted environment, as shown by higher and noisier background values in ground-level sulfur concentrations (Fig. 13). Nevertheless, some elevated values in SO_2 and SO_4 concentrations (up to 5 and 5.5 $\mu g\ m^{-3}$

5   respectively), well exceeding the SO_2 noise level, are recorded simultaneously at all three Denmark stations (Risoe, Anholt and Tange) but also much more broadly at Bredkälen (Sweden) and Pallas (Finland) at the end of October 2014 over a few days. Consequently, such an episode of atmospheric pollution could be also of volcanic origin. Therefore, we demonstrate here the large-scale impact of the Horuhraun eruption on gas and particulate air pollution by SO_2 and sulfate aerosols, affecting broadly Europe, not only France as shown in Sections 3.1 and 3.4 but also vastly Scandinavia.

     To understand the rate of SO_2 oxidation to sulfate in volcanic clouds, we also investigate the SO_2:SO_4 mass concentration ratio observed at these various EMEP stations (right of Fig. 13). For the sake of comparison, we represent in Fig. 14 the scatter plot of SO_2 versus SO_4 mass concentrations gathering data collected by ACSM and air quality stations in France (Section 3.3) during volcanic events (green and red) and background urban/agricultural conditions at SIRTA (violet stars) as well as

15   Scandinavian observations from EMEP stations. Volcanic sulfate aerosols display a clearly distinct behavior compared to the background conditions at SIRTA. In this context, SIRTA background presents low SO_4 concentration values < 2 $\mu g\ m^{-3}$ while SO_2 concentration can reach up to more than 70 $\mu g\ m^{-3}$, thus leading to a very high SO_2:SO_4 mass concentration ratio of about 50. As discussed earlier, EMEP stations in Scandinavia are located in preserved remote areas very poor in both SO_2 and SO_4, as illustrated also in Fig. 13.

20   Volcanogenic events of pollution are associated to higher sulfate concentrations, the largest event in the data presented in this article being recorded at SIRTA/France (red). They also present a relatively wide range of SO_2:SO_4 ratios, values nevertheless always lower than under SIRTA background conditions. Together with a sub-period of the largest volcanic event at SIRTA in late September 2014 (in red), strongly volcanically-influenced Northern Scandinavia EMEP stations in Sweden (Bredkälen in light blue) and Finland (Pallas-Matorova in dark blue) display the highest SO_2:SO_4 concentration ratios around 6.7. The more

25   minor volcanic event 2 recorded in France/Dunkirk in early September 2014 (green circles) shows the lowest SO_2:SO_4 ratio between 0.6 and 1, similar to those observed at poorly-volcanically-influenced Denmark stations. In between, we also observe intermediate volcanic behaviors, as illustrated by a sub-period of the largest volcanic event at SIRTA/France associated to a SO_2:SO_4 ratio of 3.1.

     To summarize, we observe a wide range of oxidation rates of SO_2 to sulfate in the Holuhraun volcanic cloud, with a SO_2:SO_4

30   mass concentration ratio in 0.6–7 strictly distinct from background sulfur speciation associated to a ratio of about 50. This significant variability attests of the complex processes that control the oxidation of SO_2 within a volcanic cloud, as developed in the following. Elevated SO_2:SO_4 ratios observed at Northern Scandinavia stations may indicate the impact on air quality of a relatively young volcanic cloud, as attested by OMPS and IASI satellite observations, which has undergone specific atmospheric conditions during its high-altitude (up to 8 kilometers) transport at high latitudes according to IASI satellite obser-

35 vations of the altitude of SO$_2$ (see Animation of IASI SO$_2$ column amount and altitude observations of the Holuhraun volcanic cloud in Sept and Oct 2014 in Supplementary Material) poorer in solar radiation and OH- radicals. On the other hand, lower SO$_2$:SO$_4$ ratios may be associated to more aged and diluted volcanic clouds, hence providing more time for SO$_2$ oxidation. These aged volcanic clouds have also probably resided a longer time at lower altitude thus meeting drastically different atmospheric conditions and more likely mixing with other types of aerosols.

4   Conclusions

Combining OMPS and IASI satellite observations with time series of ground-level mass concentrations of SO$_2$ and SO$_4$ from air quality monitoring and ACSM stations, we identify the arrival of the Holuhraun SO$_2$-rich cloud in France triggering three noteworthy episodes of volcanogenic air pollution events in Sept 2014. We explore the chemical signature of these volcanic

10 events, associated to peak values in both SO$_2$ and SO$_4$ surface abundance, through ACSM observations performed at two distant French stations that are in contrasted environmental conditions. Indeed, Dunkirk hosts vigorous harbour and industrial sulfur-rich emitting activities whereas the SIRTA site, located in the Paris suburb, is influenced by urban and agricultural activities. We highlight a chemical fingerprint of Holuhraun sulfate particles clearly distinct from background aerosols in an urban/agricultural environment, which is characterized by a pronounced depletion in nitrate and organic aerosols and only a

15 slight decrease in ammonium. Thermodynamic model simulations of Seinfeld and Pandis (2012) suggest that the elevated concentration of sulfates recorded within volcanic clouds could support this distinct chemical fingerprint of volcanic compared to background aerosols. Interestingly, volcanic sulfate aerosols in France are shown to be mostly neutralized by ammonia except when recorded in very high concentration. They can consequently be also easily isolated from freshly-emitted acidic industrial sulfates. Hence, representing scatter plots of NO$_3$:SO$_4$ and Org:SO$_4$ versus the degree of aerosol acidity allows the discrimi-

20 nation of volcanic sulfate aerosols from other types of surrounding particles.

Moreover, the joint analysis of ACSM sulfate ground-level concentration and aerosol optical depth from the AERONET sunphotometer network allowed us to demonstrate the weeks-long persistence of sulfate aerosols in the boundary layer, much longer than the lifetime of SO$_2$ of a few days at most. In addition, the exploration of SO$_2$ and SO$_4$ ground-level concentrations

25 from 19 stations of the EMEP network shows that the Holuhraun air pollution in both gas and particulate sulfate is not restricted to France but is spread more broadly in Europe up to the North of Scandinavia. A wide range of SO$_2$ oxidation to sulfate is described within volcanic clouds reflecting their complex atmospheric history.

While most air quality studies have focused on Holuhraun SO$_2$ observations and atmospheric modeling, such result suggests

30 an underestimation of the actual impact of tropospheric eruptions on air quality and health but also more broadly on climate. All the more so as the depletion in organics that we showed may also indicate the formation of organosulfate particles within the volcanic cloud, an efficient cloud condensation nuclei and climate forcing agent.

Video supplement. Two movies illustrating the Holuhraun volcanic cloud dispersal in September and October 2014 are available in the Supplement, the first including IASI SO_2 column amount and altitude observations and the second OMPS SO_2 satellite observations.

Author contributions. M. B (text, analysis and interpretation of satellite, ACSM, EMEP, air quality monitoring and AERONET data),
5   O. Favez (ACSM data acquisition at SIRTA, interpretation and contribution to text), V. Riffault (ACSM data acquisition at Dunkirk and interpretation), C. Brogniez (discussions on the overall manuscript), J. Sciare (ACSM data acquisition at SIRTA), I. Chiapello (analysis of AERONET AOD timeseries at Dunkirk and SIRTA), L. Clarisse (processing of IASI SO_2 observations), S. Zhang (initial processing of ACSM data in Dunkirk, air quality monitoring data acquisition at Dunkirk Port-East station), N. Pujol-Sohne (air quality monitoring data acquisition in Hauts de France region), E. Tison (ACSM data acquisition at Dunkirk), H. Delbarre and P. Goloub (PIs of the AERONET data
10 acquitision at Dunkirk and SIRTA respectively).

Competing interests. No competing interests.

Acknowledgements. M. B, I. C and C. B gratefully acknowledge support from the French National Research Agency (ANR) for funding the VOLCPLUME project (ANR-15-CE04-0003-01) and the Chantier Arctique for funding the PARCS project (Pollution in the ARCtic System). This work is a contribution to the CaPPA project (Chemical and Physical Properties of the Atmosphere), funded by the ANR through the PIA
15 (Programme d'Investissement d'Avenir) under contract ANR-11-LABX-0005-01 and by the Regional Council of Hauts-de-France and the European Funds for Regional Economic Development (FEDER) and to the CPER Climibio program. Aerosol measurements at SIRTA have been performed in the frame of the EU-FP7 and H2020 ACTRIS projects (grant agreements no. 262254 and 654109). They are also supported by CNRS and the Ministry of Environment through the French reference laboratory for air quality monitoring (LCSQA). L.C. is a research associate, supported by the Belgian F.R.S.-FNRS. Researchers and agencies in charge of air quality monitoring networks (Atmo NPDC
20 (now Atmo Hauts-de-France), Airparif and EMEP) provided invaluable observations and are gratefully thanked. In particular, we thank the following EMEP data providers: U. Makkonen and M. Vestenius (Finnish Meteorological Institute, FMI, Atmospheric Composition Unit, Helsinki, Finland) for Pallas-Matorova station in Finland; W. Aas and A. Hjellbrekke (Norwegian Institute for Air Research, NILU, Atmosphere and Climate Department, Kjeller, Norway) for Tustervatn station in Norway; K. Sjoberg (Swedish Environmental Research Institute, IVL, Gteborg, Sweden) for Bredkälen station in Sweden; T. Ellermann, C. Monies and R. Keller (Aarhus Universitet, ATAIR,
25 ENVIS, Roskilde, Denmark) for Risoe, Anholt and Tange stations in Denmark. We thank H. Delbarre and P. Goloub for their efforts in establishing and maintaining Dunkirk and Palaiseau AERONET sites. NASA Goddard Earth Sciences Data and Information Services Center (GES DISC) are acknowledged for providing OMPS satellite SO_2 total column data. The French Government Geoportail is thanked for having provided an aerial image of Dunkirk through its public website (https://www.geoportail.gouv.fr).

References

Aas, W., Solberg, S., and Yttri, K.: Monitoring of long-range transported air pollutants in Norway, Annual Report M-203, NILU, 2013.

Allen, A. G., Oppenheimer, C., Ferm, M., Baxter, P. J., Horrocks, L. A., Galle, B., ..., Duffell, H. J. . P. s. a., and associated emissions from
   Masaya Volcano, Nicaragua. Journal of Geophysical Research: Atmospheres, D.: Allen, A. G. and Oppenheimer, C. and Ferm, M. and
   Baxter, P. J. and Horrocks, L. A. and Galle, B. and ... and Duffell, H. J., Journal of Geophysical Research: Atmospheres, 107, 2002.

Bauduin, S., Clarisse, L., Clerbaux, C., Hurtmans, D., and Coheur, P.-F.: IASI observations of sulfur dioxide (SO2) in the boundary layer of
   Norilsk, J. Geophys. Res., 119, 4253–4263, https://doi.org/10.1002/2013JD021405, 2014.

Boichu, M., Chiapello, I., Brogniez, C., Péré, J.-C., Thieuleux, F., Torres, B., Blarel, L., Mortier, A., Podvin, T., Goloub, P., Söhne, N.,
   Clarisse, L., Bauduin, S., Hendrick, F., Theys, N., Van Roozendael, M., and Tanré, D.: Current challenges in modelling far-range air
   pollution induced by the 2014-2015 Bárðarbunga fissure eruption (Iceland), Atmos. Chem. Phys., 2016.

Boichu, M., Brogniez, C., Chiapello, I., Blarel, L., Torres, B., Derimian, Y., Goloub, P., and Tanré, D.: Impact of the Holuhraun flood lava
   eruption at Bardarbunga volcano (Iceland, 2014–15) on optical, microphysical and radiative properties of aerosols in Europe, Atm. Chem.
   Phys. Discuss., 2019 in prep.

Boulon, J., Sellegri, K., Hervo, M., and Laj, P.: Observations of nucleation of new particles in a volcanic plume., Proceedings of the National
   Academy of Sciences, 108, 12 223–12 226, 2011.

Budisulistiorini, S. H., Canagaratna, M. R., Croteau, P. L., Baumann, K., Edgerton, E. S., Kollman, M. S., Ng, N. L., Verma, V., Shaw, S. L.,
   Knipping, E. M., Worsnop, D. R., Jayne, J. T., Weber, R. J., and Surratt, J. D.: Intercomparison of an Aerosol Chemical Speciation Monitor
   (ACSM) with ambient fine aerosol measurements in downtown Atlanta, Georgia, Atmos. Meas. Tech., 7, 1929–1941, 2014.

Carn, S., Krueger, A., Krotkov, N., Yang, K., and Evans, K.: Tracking volcanic sulfur dioxide clouds for aviation hazard mitigation, Nat.
   Hazards, 51, 325–343, https://doi.org/10.1007/s11069-008-9228-4, 2009.

Carn, S. A., Yang, K., Prata, A. J., and N.A.Krotkov: Extending the long-term record of volcanic SO$_2$ emissions with the Ozone Mapping
   and Profiler Suite nadir mapper, Geophys. Res. Lett., 42, 2015.

Clarisse, L., Coheur, P.-F., Theys, N., Hurtmans, D., and Clerbaux, C.: The 2011 Nabro eruption, a SO$_2$ plume height analysis using IASI
   measurements, Atmos. Chem. Phys., 14, 3095–3111, 2014.

Clerc, F., Douchez, C., Gibaux, J.-P., Dedourge, J.-M., Chanu, G., and Mathon, M.-P.: L'industrie au regard de l'environnement en Nord–
   Pas–de–Calais, Tech. rep., DREAL (Direction régionale de l'environnement, de l'aménagement et du logement)– Nord-Pas-de-Calais,
   2012.

Crenn, V., Sciare, J., Croteau, P. L., Verlhac, S., Fröhlich, R., Belis, C. A., Aas, W., Äijälä, M., Alastuey, A., Artiñano, B., Baisnée, D.,
   Bonnaire, N., Bressi, M., Canagaratna, M., Canonaco, F., Carbone, C., Cavalli, F., Coz, E., Cubison, M. J., Esser-Gietl, J. K., Green, D. C.,
   Gros, V., Heikkinen, L., Herrmann, H., Lunder, C., Minguillòn, M. C., Mocnik, G., O'Dowd, C. D., Ovadnevaite, J., Petit, J. E., Petralia,
   E., Poulain, L., Priestman, M., Riffault, V., Ripoll, A., Sarda-Estève, R., Slowik, J. G., Setyan, A., Wiedensohler, A., Baltensperger, U.,
   Prévôt, A. S. H., Jayne, J. T., and Favez, O.: ACTRIS ACSM intercomparison – Part 1: Reproducibility of concentration and fragment
   results from 13 individual Quadrupole Aerosol Chemical Speciation Monitors (Q-ACSM) and consistency with co-located instruments,
   Atmos. Meas. Tech., 8, 5063–5087, 2015.

Delmelle, P.: Environmental impacts of tropospheric volcanic gas plumes, Geological Society, London, Special Publications, 213, 381–400,
   2003.

Ebmeier, S., Sayer, A., Grainger, R., Mather, T., and Carboni, E.: Systematic satellite observations of the impact of aerosols from passive volcanic degassing on local cloud properties, Atmosph. Chem. Phys., 14, 10 601–10 618, https://doi.org/10.5194/acp-14-10601-2014, 2014.

5 Freney, E., Zhang, Y., Croteau, P., Amodeo, T., Williams, L., Truong, F., Petit, J.-E., Sciare, J., Sarda-Estève, R., Bonnaire, N., Crenn, V., Arumae, T., Aurela, M., Bougiatioti, K., Coz, E., Elste, T., Heikkinen, L., Minguillon, M.-C., Poulain, L., Priestman, M., Stavroulas, I., Tobler, A., Vasilescu, J., Zanca, N., Alastuey, A., Artinano, B., Carbone, C., Flentje, H., Green, D., Herrmann, H., Maasikmets, M., Marmureanu, L., Prévôt, A. S. H., Wiedensohler, A., Canagaratna, M., Gros, V., Jayne, J. T., and Favez, O.: The second ACTRIS inter-comparison (2016) for Aerosol Chemical Speciation Monitors (ACSM): Calibration protocols and instrument performance evaluations,
10 Aerosol Sci. Technol., subm.

Gassó, S.: Satellite observations of the impact of weak volcanic activity on marine clouds, Journal of Geophysical Research (Atmospheres), 113, 2008.

Haeffelin, M., Barthès, L., Bock, O., Boitel, C., Bony, S., Bouniol, D., Chepfer, H., Chiriaco, M., Cuesta, J., Delanoë, J., Drobinski, P., Dufresne, J. L., Flamant, C., Grall, M., Hodzic, A., Hourdin, F., Lapouge, F., Lemaître, Y., Mathieu, A., Morille, Y., Naud, C., Noël, V.,
15 O'Hirok, W., Pelon, J., Pietras, C., Protat, A., Romand, B., Scialom, G., and Vautard, R.: SIRTA, a ground-based atmospheric observatory for cloud and aerosol research, Ann. Geophys., 23, 253–275, 2005.

Hatakka, J., Aalto, T., Aaltonen, V., Aurela, M., Hakola, H., Komppula, M., ., and Viisanen, Y.: Overview of the atmospheric research activities and results at Pallas GAW station., Boreal Environment Research, 8, 365–384, 2003.

Holben, B., Smirnov, A., Eck, T., Slutsker, I., Abuhassan, N., Newcomb, W., Schafer, J., Tanre, D., Chatenet, B., and Lavenu, F.: An emerging
20 ground-based aerosol climatology- Aerosol optical depth from AERONET, J. Geophys. Res., 106, 12 067–12 097, 2001.

Ialongo, I., Hakkarainen, J., Kivi, R., Anttila, P., Krotkov, N., Yang, K., Li, C., Tukiainen, S., Hassinen, S., and Tamminen, J.: Validation of satellite SO_2 observations in northern Finland during the Icelandic Holuhraun fissure eruption, Atmos. Meas. Techn., 8, 2279–2289, https://doi.org/10.5194/amt-8-2279-2015, 2015.

ICAO: Volcanic Ash Contingency Plan - European and North Atlantic Regions, European and North Atlantic Office of the International Civil
25 Organization, EUR Doc 019, NAT Doc 006, Part II, 2016.

Ilyinskaya, E., Tsanev, V. I., Martin, R. S., Oppenheimer, C., Le Blond, J., Sawyer, G. M., and Gudmundsson, M. T.: Near-source observations of aerosol size distributions in the eruptive plumes from Eyjafjallajökull volcano, March–April 2010., Atmospheric Environment, 45, 3210–3216, 2011.

Kroll, J. H., Cross, E. S., Hunter, J. F., Pai, S., XII, T., TREX XI Wallace, M., Croteau, P., Jayne, J., Worsnop, D. R., Heald, C. L., Murphy,
30 J., and Frankel, S.: Atmospheric evolution of volcanic smog ("vog") from Kilauea: real-time measurements of oxidation, dilution and neutralization within a volcanic plume, Environ. Sci. Technol., 49, 4129–4137, 2015.

Krotkov, N., McClure, B., Dickerson, R., Carn, S. A., Li, C., Bhartia, P. K., Yang, K., Krueger, A., and Li, Z.: Validation of SO2 retrievals from the Ozone Monitoring Instrument over NE China, Journal of Geophysical Research, 113, 2008.

Kuebbeler, M., Lohmann, U., and Feichter, J.: Effects of stratospheric sulfate aerosol geo-engineering on cirrus clouds, Geophys. Res. Lett.,
35 39, 2012.

Longo, B., Rossignol, A., and Green, J.: Cardiorespiratory health effects associated with sulphurous volcanic air pollution, Public health, 122, 809–820, 2008.

Malavelle, F. F., Haywood, J. M., Jones, A., Gettelman, A., Clarisse, L., Bauduin, S., Allan, R., Karset, I., Kristjansson, J., Oreopoulous, L., Cho, N., Lee, D., Bellouin, N., Boucher, O., Grosvenor, D., Carslaw, K., Dhomse, S., Mann, G., Schmidt, A., Coe, H., Hartley, M., Dalvi,

M., Hill, A., Johnson, B. T., Johnson, C., Knight, J., O'Connor, F., Partridge, D., Stier, P., Myhre, G., Platnick, S., Stephens, G., Takahashi, H., and Thordarson, T.: Strong constraints on aerosol–cloud interactions from volcanic eruptions., Nature, 546, 485, 2017.

Martin, R. S., Ilyinskaya, E., Sawyer, G. M., Tsanev, V. I., and Oppenheimer, C.: A re-assessment of aerosol size distributions from Masaya
5 volcano (Nicaragua)., Atmospheric environment, 45, 547–560, 2011.

Mather, T. A., Allen, A. G., Oppenheimer, C., Pyle, D. M., and McGonigle, A. J. S.: Size-resolved characterisation of soluble ions in the particles in the tropospheric plume of Masaya volcano, Nicaragua: Origins and plume processing., Journal of Atmospheric Chemistry, 46, 207–237, 2003a.

Mather, T. A., Pyle, D. M., and Oppenheimer, C.: Tropospheric volcanic aerosol., Geophysical Monograph-American Geophysical Union,
10 139, 189–212, 2003b.

Mather, T. A., Tsanev, V. I., Pyle, D. M., McGonigle, A. J. S., Oppenheimer, C., and Allen, A. G.: Characterization and evolution of tropospheric plumes from Lascar and Villarrica volcanoes, Chile., Journal of Geophysical Research: Atmospheres, 109, 2004.

McCoy, D. T. and Hartmann, D. L.: Observations of a substantial cloud-aerosol indirect effect during the 2014–2015 Bárðarbunga-Veiðivötn fissure eruption in Iceland, Geophysical Research Letters, 42, 10 409–10 414, 2015.

15 Middlebrook, A. M., Bahreini, R., Jimenez, J. L., and Canagaratna, M. R.: Evaluation of Composition-Dependent Collection Efficiencies for the Aerodyne Aerosol Mass Spectrometer using Field Data, Aerosol Sci. Tech., 46, 258–271, 2012.

Neely, R., Toon, O., Solomon, S., Vernier, J.-P., Alvarez, C., English, J., Rosenlof, K., Mills, M., Bardeen, C., Daniel, J., et al.: Recent anthropogenic increases in SO_2 from Asia from Asia have minimal impact on stratospheric aerosol, Geophys. Res. Lett., 40, 999–1004, 2013.

20 Ng, N. L., Herndon, S. C., Trimborn, A., Canagaratna, M. R., Croteau, P. L., Onasch, T. B., Sueper, D., Worsnop, D. R., Zhang, Q., Sun, Y. L., and Jayne, J. T.: An Aerosol Chemical Speciation Monitor (ACSM) for Routine Monitoring of the Composition and Mass Concentrations of Ambient Aerosol, Aerosol Science and Technology, 45, 780–794, 2011.

Oppenheimer, C., Scaillet, B., and Martin, R.: Sulfur Degassing From Volcanoes: Source Conditions, Surveillance, Plume Chemistry and Earth System Impacts, Reviews in Mineralogy and Geochemistry, 73, 363–421, 2011.

25 Pattantyus, A., Businger, S., and Howell, S.: Review of sulfur dioxide to sulfate aerosol chemistry at Kilauea Volcano, Hawai'i, Atmospheric Environment, 185, 262–271, 2018.

Petit, J.-E., Petit, J.-E., Favez, O., Sciare, J., Crenn, V., Sarda-Estève, R., Bonnaire, N., Mocnik, G., Dupont, J.-C., Haeffelin, M., and Leoz-Garziandia, E.: Two years of near real-time chemical composition of submicron aerosols in the region of Paris using an Aerosol Chemical Speciation Monitor (ACSM) and a multi-wavelength Aethalometer, Atmos. Chem. Phys., 15, 2985–3005, 2015.

30 Radke, L.: Chlorine, fluorine, and sulfur emissions from Mount Erebus, Antarctica and estimated contributions to the Antarctic atmosphere., Nature, 299, 710 – 712, 1982.

Ridley, D., Solomon, S., Barnes, J., Burlakov, V., Deshler, T., Dolgii, S., Herber, A. B., Nagai, T., Neely, R., Nevzorov, A., et al.: Total volcanic stratospheric aerosol optical depths and implications for global climate change, Geophysical Research Letters, 2014.

Robock, A.: Volcanic eruptions and climate, Reviews of Geophysics, 38, 191–220, https://doi.org/10.1029/1998RG000054, 2000.

35 Santer, B. D., Bonfils, C., Painter, J. F., Zelinka, M. D., Mears, C., Solomon, S., Schmidt, G. A., Fyfe, J. C., Cole, J. N., Nazarenko, L., et al.: Volcanic contribution to decadal changes in tropospheric temperature, Nature Geoscience, 7, 185–189, 2014.

Schill, G. and Tolbert, M.: Heterogeneous ice nucleation on phase-separated organic-sulfate particles: effect of liquid vs. glassy coatings, Atm. Chem. Phys., 13, 4681–4695, 2013.

Schlag, P., Rubach, F., Mentel, T. F., Reimer, D., Canonaco, F., Henzing, J. S., Moerman, M., Otjes, R., Prevot, A., Rohrer, F., Rosati, B., Tillmann, R., Weingartner, E., and Kiendler-Scharr, A.: Ambient and laboratory observations of organic ammonium salts in PM$_1$, Faraday Discuss., 200, 331–351, 2017.

5 Schmidt, A., Carslaw, K. S., Mann, G. W., Rap, A., Pringle, K. J., Spracklen, D. V., Wilson, M., and Forster, P. M.: Importance of tropospheric volcanic aerosol for indirect radiative forcing of climate, Atmosph. Chem. Phys., 12, 7321–7339, https://doi.org/10.5194/acp-12-7321-2012, 2012.

Schmidt, A., Leadbetter, S., Theys, N., Carboni, E., Witham, C. S., Stevenson, J. A., Birch, C. E., Thordarson, T., Turnock, S., Barsotti, S., Delaney, L., Feng, W., Grainger, R. G., Hort, M. C., Höskuldsson, Á., Ialongo, I., Ilyinskaya, E., Jóhannsson, T., Kenny, P., Mather, T. A.,

10 Richards, N. A. D., and Shepherd, J.: Satellite detection, long-range transport, and air quality impacts of volcanic sulfur dioxide from the 2014–2015 flood lava eruption at Bárðarbunga (Iceland), J. Geophys. Res. Atm., 120, 9739–9757, 2015.

Seinfeld, J. and Pandis, S. N.: Atmospheric chemistry and physics: from air pollution to climate change., John Wiley and Sons, 2012.

Solomon, S., Daniel, J., Neely, R., Vernier, J.-P., Dutton, E., and Thomason, L.: The persistently variable background stratospheric aerosol layer and global climate change, Science, 333, 866–870, 2011.

15 Steensen, B., Schulz, M., Theys, N., and Fagerli, H.: A model study of the pollution effects of the first 3 months of the Holuhraun volcanic fissure: comparison with observations and air pollution effects, Atm. Chem. Phys., 16, 9745–9760, 2016.

Stevenson, D., Johnson, C., Collins, W., and Derwent, R.: The tropospheric sulphur cycle and the role of volcanic SO$_2$, Geological Society, London, Special Publications, 213, 295–305, 2003.

Targino, A. C., Krecl, P., Johansson, C., Swietlicki, E., Massling, A., Coraiola, G. C., and Lihavainen, H.: Deterioration of air quality across

20 Sweden due to transboundary agricultural burning emissions., Boreal Environment Research, 18, 19–36, 2013.

Thordarson, T. and Self, S.: Atmospheric and environmental effects of the 1783-1784 Laki eruption: A review and reassessment, J. Geophys. Res., 108, 4011, https://doi.org/10.1029/2001JD002042, 2003.

Tørseth, K., Aas, W., Breivik, K., Fjæraa, A. M., Fiebig, M., Hjellbrekke, A. G., Myhre, C. L., Solberg, S., and Yttri, K. E.: Introduction to the European Monitoring and Evaluation Programme (EMEP) and Observed Atmospheric Composition Change during 1972–2009,

25 Atmospheric Chemistry and Physics, 12, 5447–5481, 2012.

Tu, F., Thornton, D., Bandy, A., Carmichael, G., Tang, Y., Thornhill, K., Sachse, G., and Blake, D.: Long-range transport of sulfur dioxide in the central Pacific, Journal of Geophysical Research (Atmospheres), 109, 2004.

van Manen, S. M.: Perception of a chronic volcanic hazard: persistent degassing at Masaya volcano, Nicaragua, J. Appl. Volcanol., 3, 1–16, 2014.

30 Vernier, J.-P., Thomason, L. W., Pommereau, J.-P., Bourassa, A., Pelon, J., Garnier, A., Hauchecorne, A., Blanot, L., Trepte, C., Degenstein, D., and Vargas, F.: Major influence of tropical volcanic eruptions on the stratospheric aerosol layer during the last decade, Geophys. Res. Lett., 38, 12 807, https://doi.org/10.1029/2011GL047563, 2011.

von Glasow, R. and Crutzen, P.: Tropospheric Halogen Chemistry, in: Treatise on Geochemistry - The Atmosphere, edited by Keeling, R., Holland, H., and Turekion, K., vol. 4, p. 347, Oxford: Elsevier/Pergamon, 2003.

35 Xu, W., Lambe, A., Silva, P., Hu, W., Onasch, T., Williams, L., Croteau, P., Zhang, X., Renbaum-Wolff, L., Fortner, E., Jimenez, J. L., Jayne, J. T., Worsnop, D., and Canagaratna, M.: Laboratory evaluation of species-dependent relative ionization efficiencies in the Aerodyne Aerosol Mass Spectrometer, Aerosol Sci. Technol., 52, 626–641, 2018.

Yuan, T., Remer, L., and Yu, H.: Microphysical, macrophysical and radiative signatures of volcanic aerosols in trade wind cumulus observed by the A-Train, Atmosph. Chem. Phys., 2011.

Zelenski, M., Taran, Y., and Galle, B.: High emission rate of sulfuric acid from Bezymianny volcano, Kamchatka., Geophysical Research Letters, 42, 7005–7013, 2015.

Zhang, S.: Analyse dynamique, en champ proche et à résolution temporelle fine, de l'aérosol submicronique en situation urbaine sous influence industrielle, Ph.D. thesis, Université du Littoral Côte d'Opale, 2016.
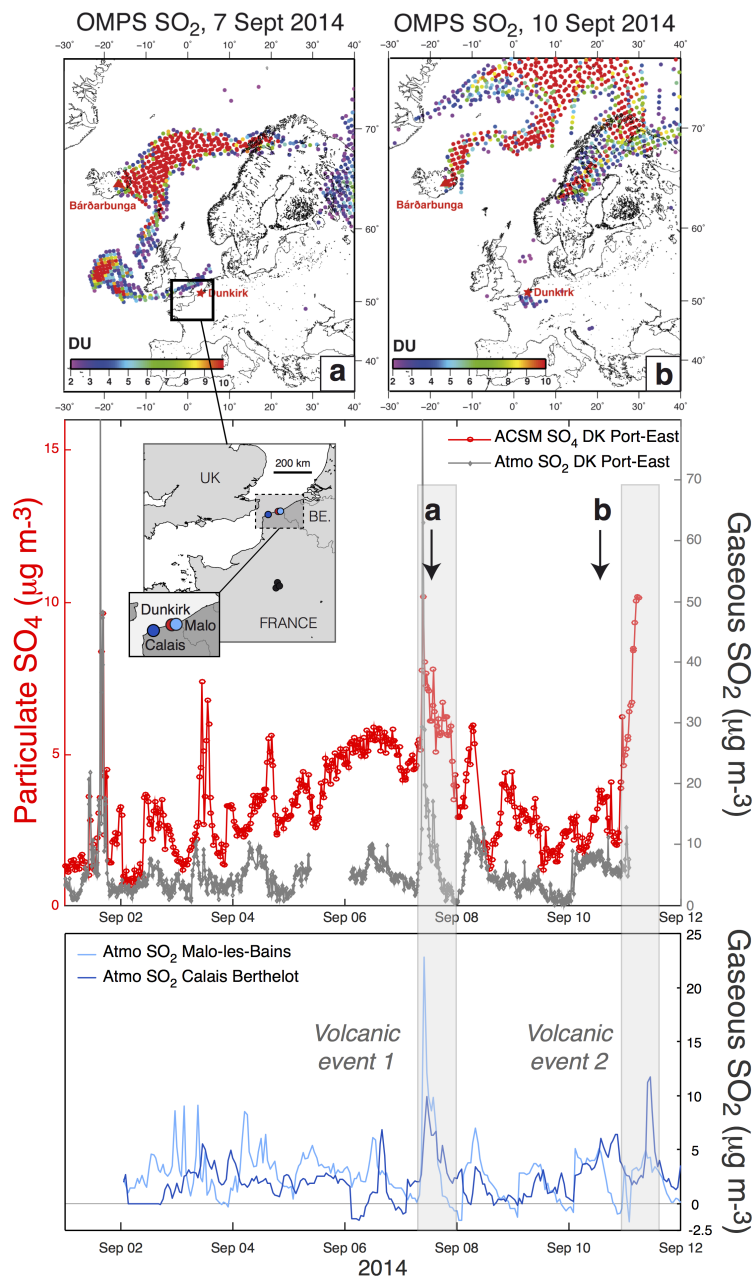
Figure 1. (Top) OMPS L2 PBL observations (1:30 PM local time at Equator) showing volcanic SO_2 from Holuhraun eruption transported over northern France early Sept 2014. (Middle) Time series of ground-level mass concentrations of (red) particulate SO_4 from 30-min resolved ACSM and (grey) gaseous SO_2 from 15-min resolved air quality measurements at Dunkirk (Port-East). Map of all stations in inset. (Bottom) Hourly time series of SO_2 mass concentration from regional neighbor stations of Malo-les-Bains (light blue) and Calais-Berthelot (dark blue) belonging to the Atmo Hauts-de-France air quality network. Note the end of ACSM SO_4 data collection on 11 Sept 14 at 05:50 UTC and the absence of valid SO_2 data after 02:00 on the same day.
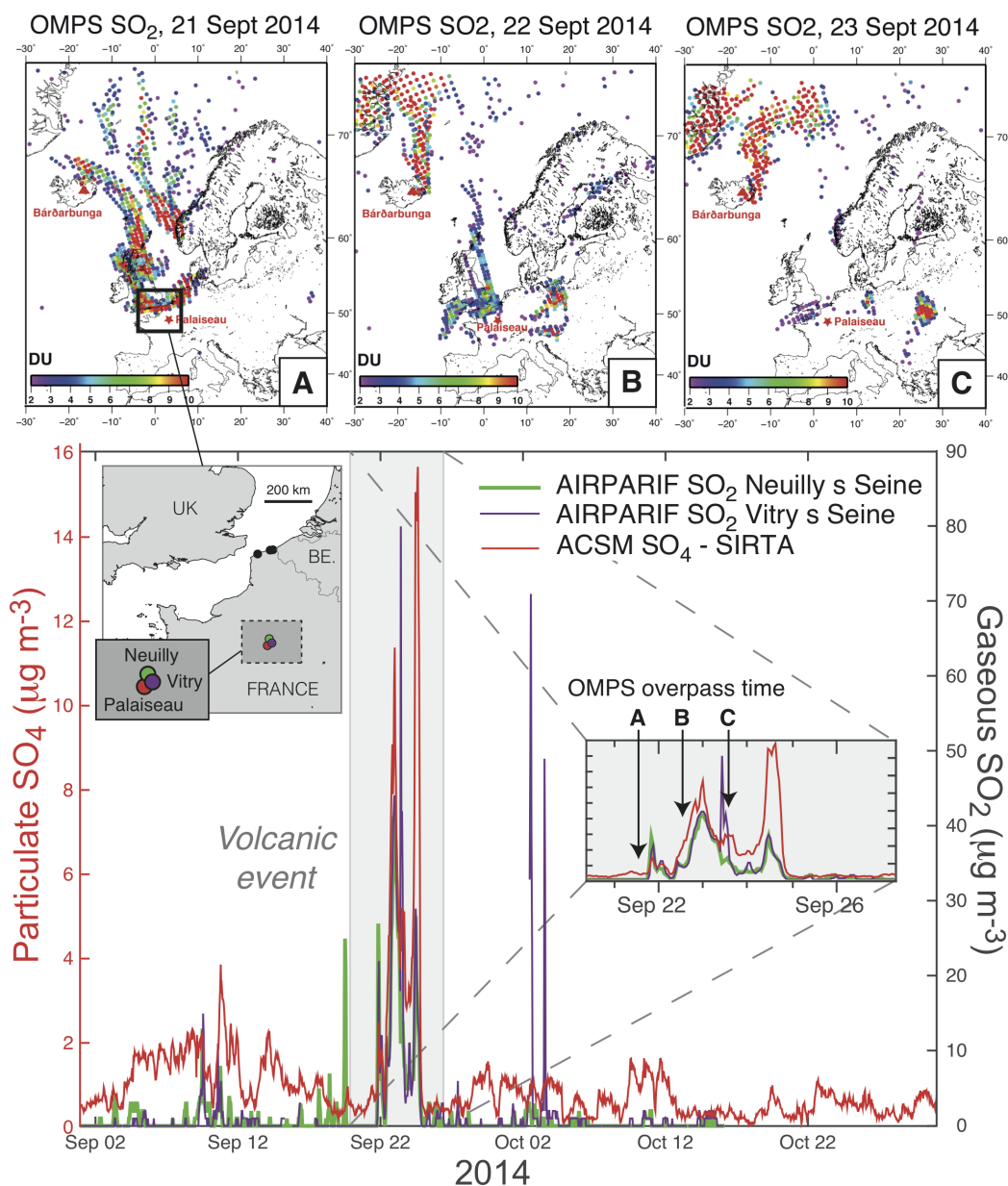
Figure 2. (Top) OMPS L2 PBL observations (1:30 PM local time at Equator) showing volcanic SO_2 from Holuhraun eruption transported over northern France in late Sept 2014. (Bottom) Hourly time series covering Sept-Oct 2014 of ground-level mass concentrations of (red) particulate SO_4 from ACSM at SIRTA and (green and purple) gaseous SO_2 from regional neighbor stations of Vitry-sur-Seine and Neuilly-sur-Seine belonging to the Airparif air quality monitoring network (station location indicated in map). In inset, a zoom on the period 19-26 Sept 2014 when the largest episode of volcanogenic air pollution in France takes place.
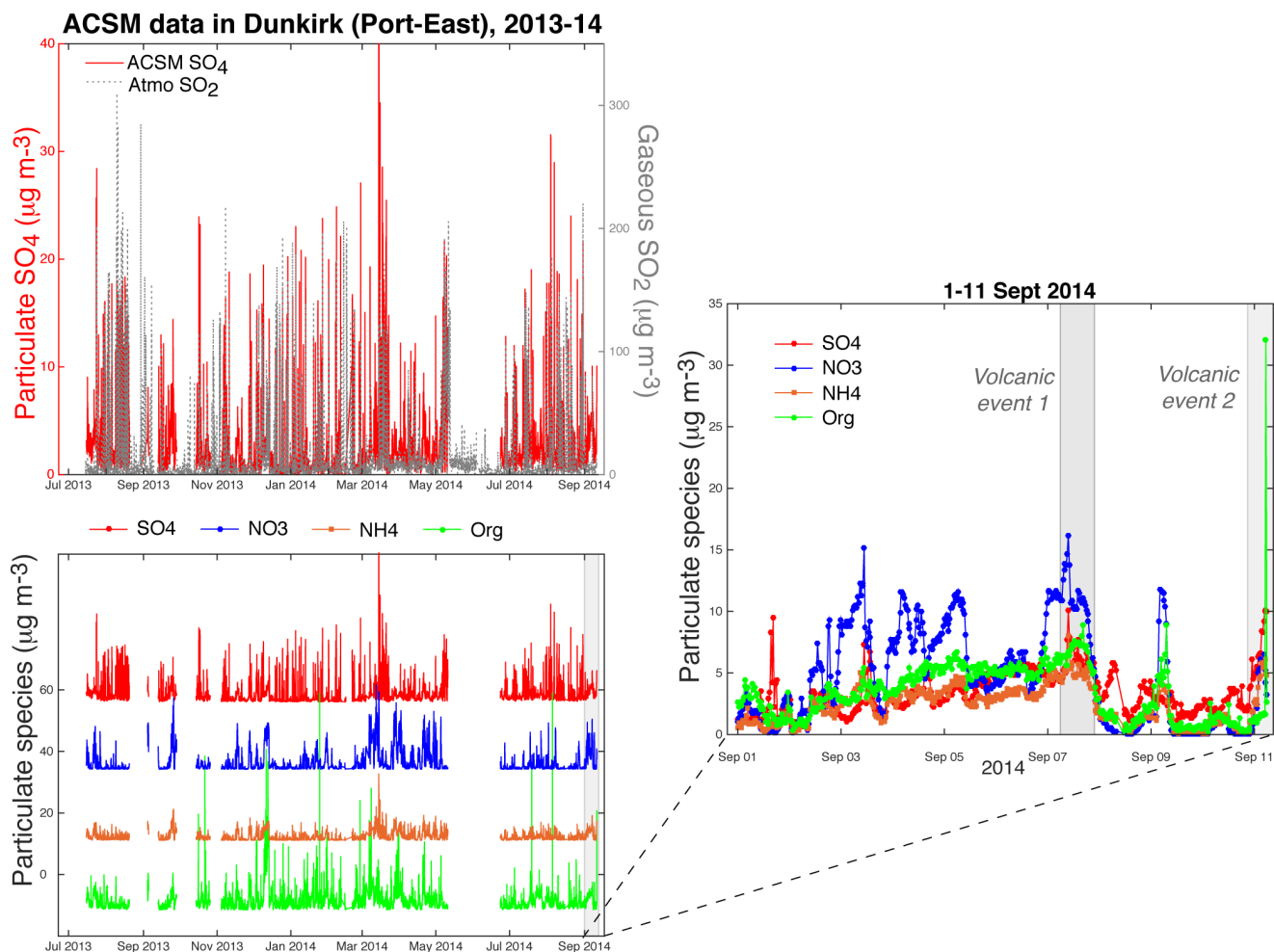
Figure 3. 14 month-long time series of (Top) (left-red) particulate SO_4 (ACSM), (right-grey) gaseous SO_2 (Atmo Hauts-de-France air quality station) and (middle) ACSM species (sulfate (SO_4), nitrate (NO_3), ammonium (NH_4) and organic (Org) aerosols) mass concentrations from 15 July 2013 until 11 Sept 2014, at Dunkirk Port-East station. (Bottom) Focus on the period 1-11 Sept 2014 when events of air pollution induced by the Holuhraun eruption were recorded.
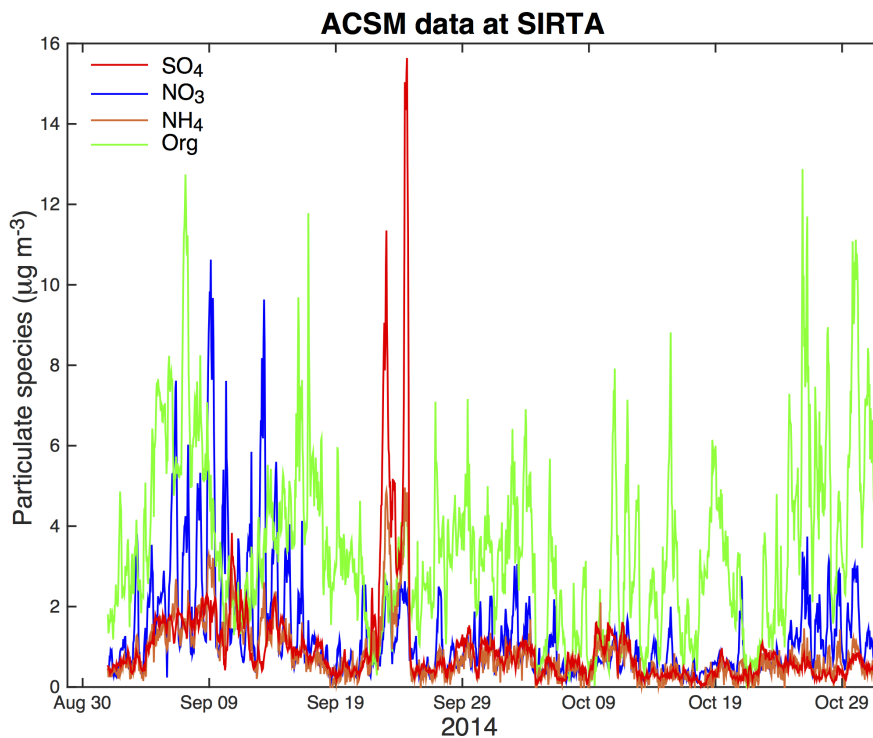
Figure 4. Two month-long time series of the mass concentration of species measured with ACSM (SO$_4$ in red, NO$_3$ in blue, NH$_4$ in orange, Org in green) at SIRTA covering the period Sept-Oct 2014 that is punctuated by volcanogenic events of air pollution in France.
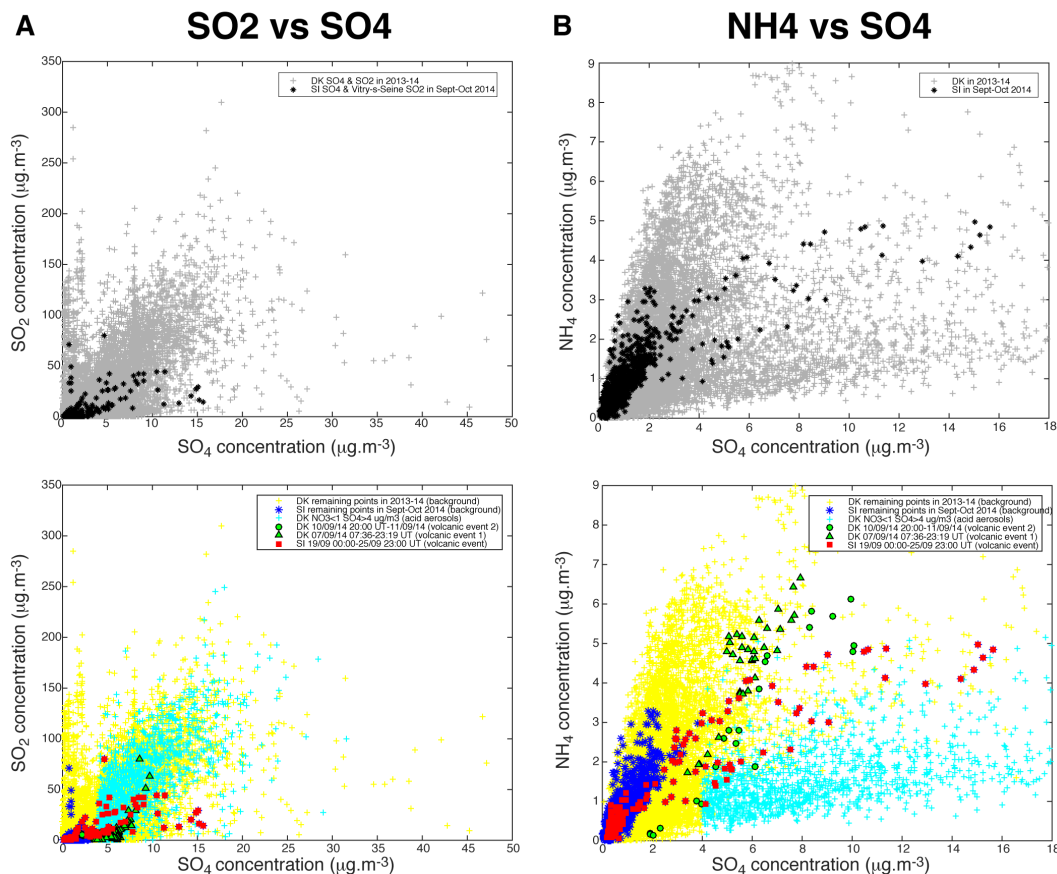
Figure 5. Scatter plots of (A) SO_2 (from Atmo Hauts-de-France station in Dunkirk or Airparif Vitry-sur-Seine station nearby SIRTA), (B) ACSM NH_4, (C) ACSM NO_3, (D) ACSM Org, vs. ACSM SO_4 mass concentrations. (Top) All available data at Dunkirk/Port-East (DK) over 15 Jul 2013-11 Sept 2014 (grey), and at SIRTA (SI) and nearby Vitry-sur-Seine Airparif station for SO_2 over 1 Sept-31 Oct 2014 (black). (Bottom) Red squares: SI data over 19 Sept 2014 00:00 – 25 Sept 2014 23:00 UT (volcanic event), green triangles: DK data over 7 Sept 2014 07:36-23:19 UT (volcanic event 1), green circles: DK data over 10 Sept 2014 20:00 UT – 11 Sept 2014 (end of data) (volcanic event 2), cyan crosses: DK data with mass concentrations of $NO_3 < 1$ and $SO_4 > 4$ μg m^{-3} (acidic aerosols), blue stars: SI remaining data (background), yellow crosses: DK remaining data (background).
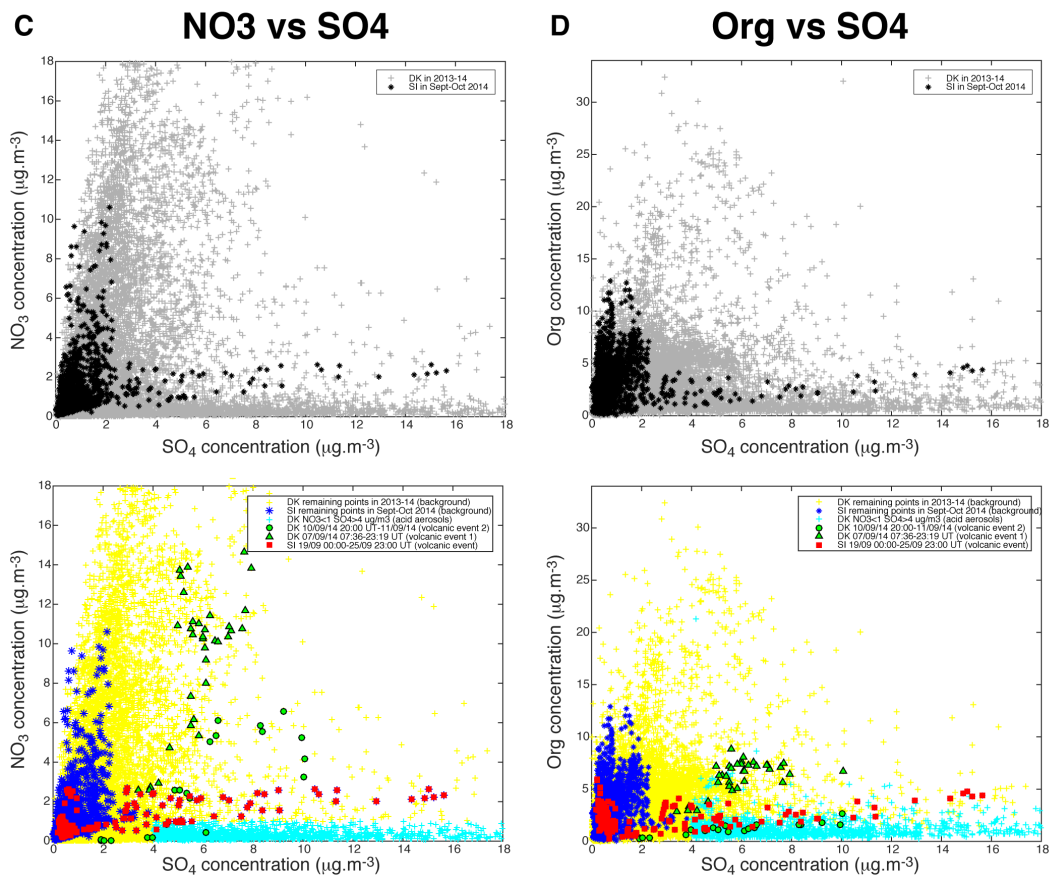
Figure 6. Same as Figure 5 but for (C) ACSM NO_3 and (D) ACSM Org vs. ACSM SO_4 mass concentrations.
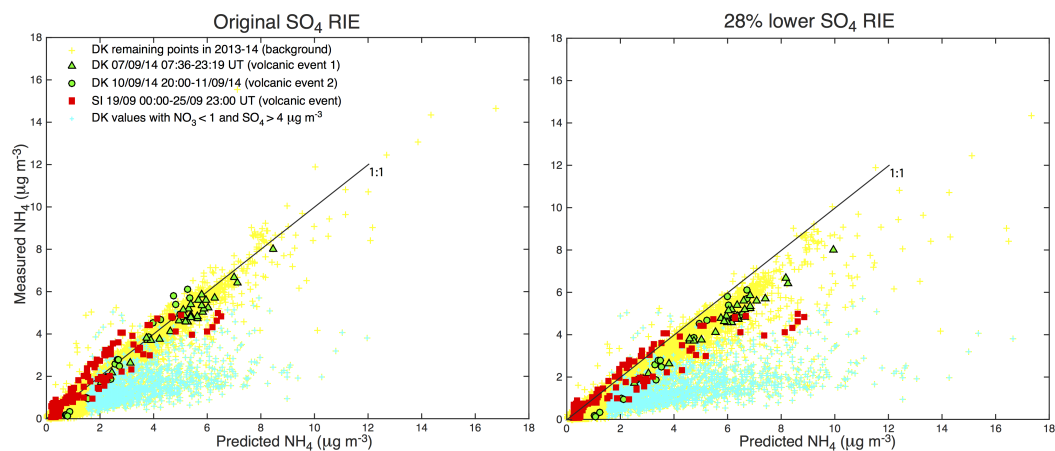
Figure 7. Scatter plot of measured (ACSM) NH_4 *versus* predicted NH_4 mass concentration for the three volcanic events of air pollution recorded at SIRTA (in red) and Dunkirk/Port-East (in green, triangles and circles for volcanic events 1 and 2 respectively) in Sept 2014. Data in cyan indicate values associated to aerosols with concentrations of $NO_3 < 1$ and $SO_4 > 4$ μg m^{-3}. Yellow data correspond to the remaining ACSM values recorded in Dunkirk over 2013–14, referring to background conditions. (Left) Original and (right) 28% lower sulfate RIE coefficients.
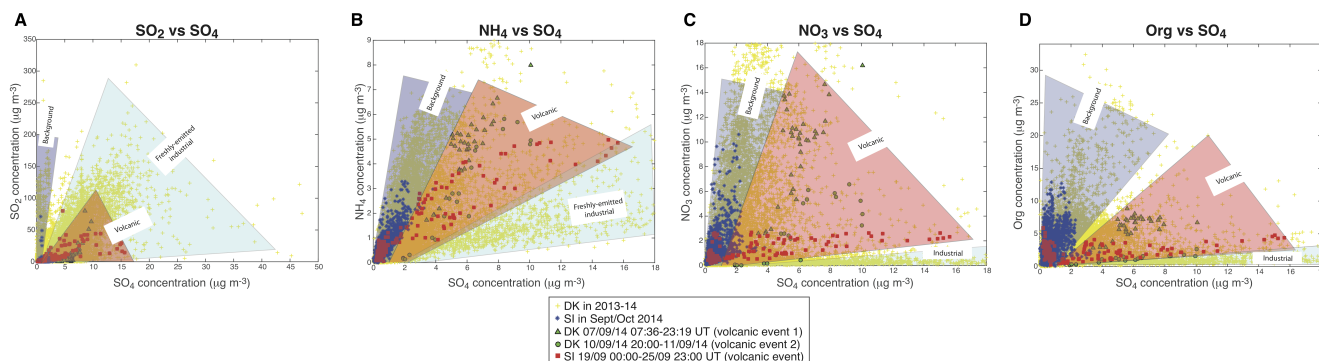
Figure 8. Distinction of aerosol sources, either representative of background conditions (blue), of volcanic (red) or industrial (cyan) origins, in the scatter plots of: (A) gaseous SO_2 from air quality stations, and various ACSM particulate species: (B) NH_4, (C) NO_3 and (D) Org, *versus* ACSM sulfate mass concentrations.
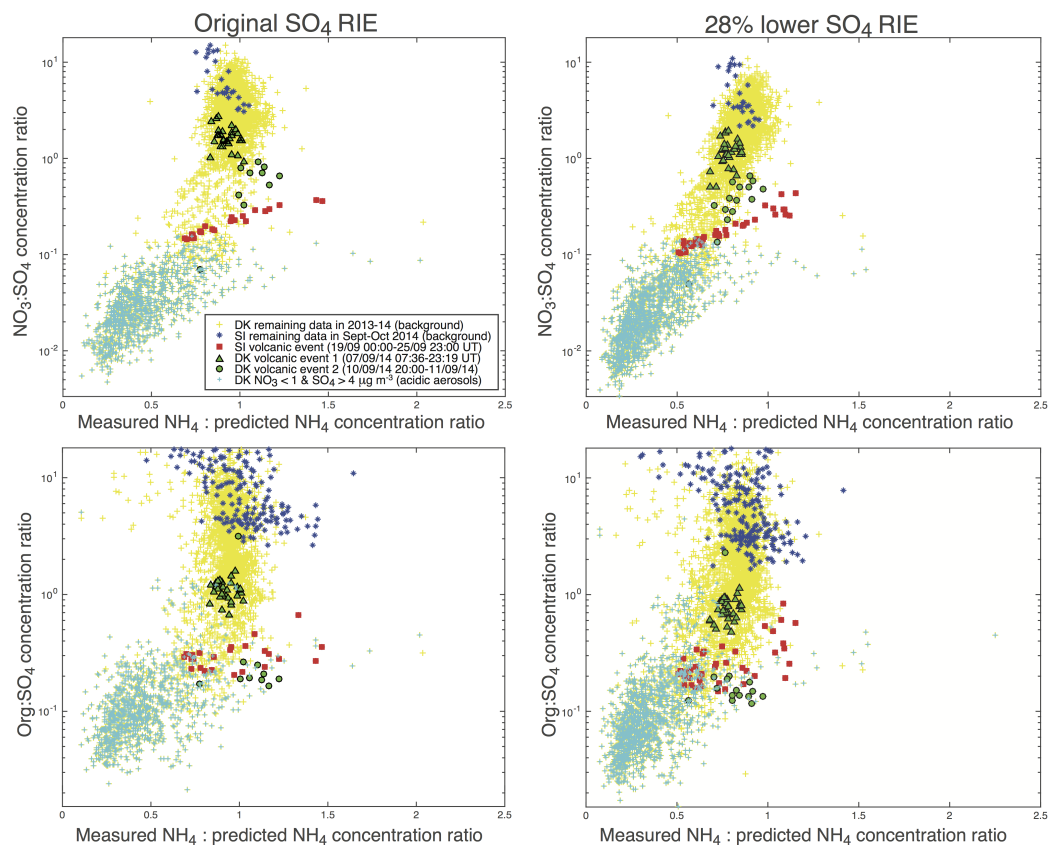
Figure 9. Scatter plots of (Top) $NO_3:SO_4$ or (Bottom) $Org:SO_4$ mass concentration ratios (in logarithmic scale) *versus* the ratio of measured to predicted NH_4 concentrations for (left) original and (right) 28% lower sulfate RIE coefficients.
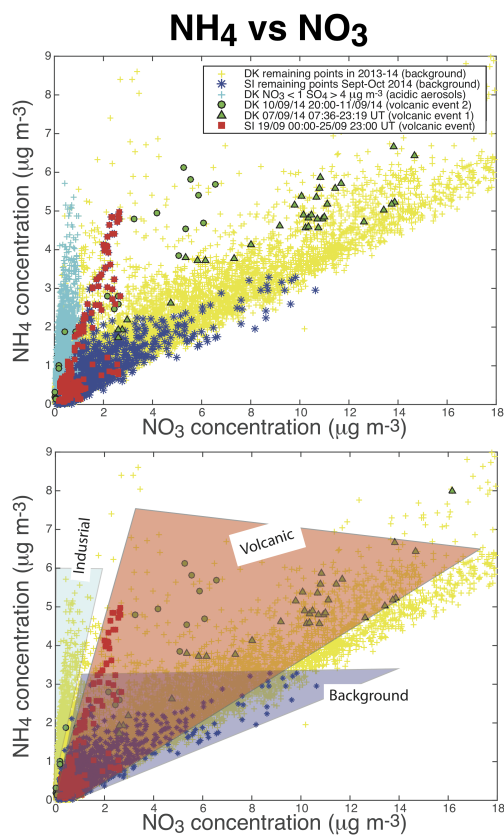
Figure 10. Scatter plot of ACSM NH$_4$ *versus* NO$_3$ mass concentrations at Dunkirk/Port-East (DK) over 15 Jul 2013-11 Sept 2014 and at SIRTA (SI) over 1 Sept-31 Oct 2014. (Top) Red squares: SI data over 19 Sept 2014 00:00 UT-25 Sept 2014 23:00UT (volcanic event), green triangles: DK data over 7 Sept 2014 07:36-23:19 UT (volcanic event 1), green circles: DK data over 10 Sept 2014 20:00 UT-11 Sept 2014 (end of data) (volcanic event 2), cyan crosses: DK data with mass concentrations of NO$_3$ < 1 and SO$_4$ > 4 μg m^{-3} (acidic aerosols), blue stars: SI remaining data (background), yellow crosses: DK remaining data (background). (Bottom) Distinction of aerosol sources.
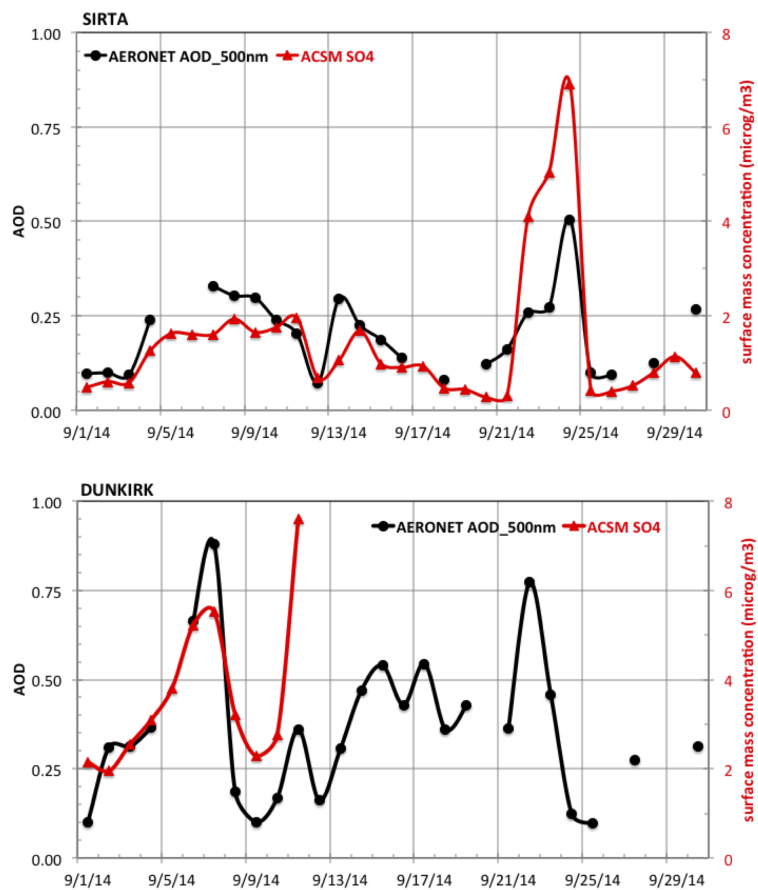
Figure 11. Time series of mean daily AERONET AOD at 500 nm and ACSM SO$_4$ mass concentration at (Top) SIRTA and (Bottom) Dunkirk.
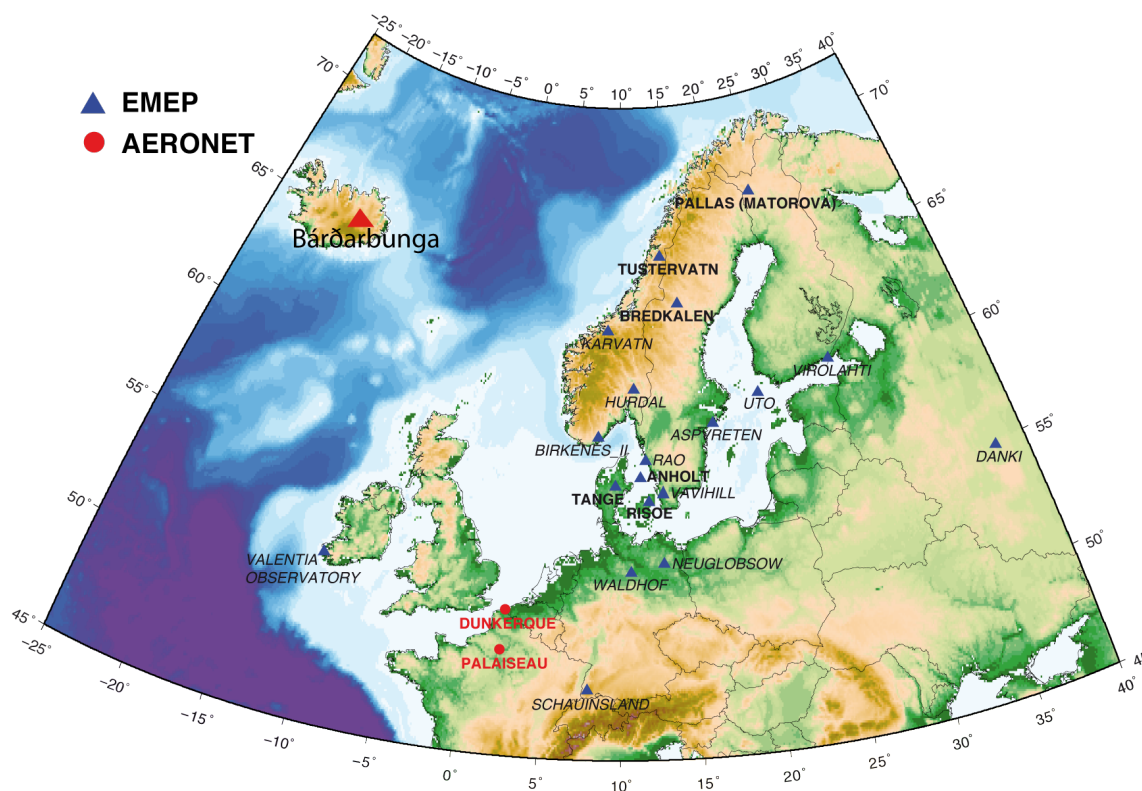
Figure 12. Map of investigated 19 EMEP stations (blue triangles). Stations with name in bold were clearly impacted by the Holuhraun eruption (with a few daily SO_2 concentrations higher than 3 μg m^{-3} over the period Sept 2014–Feb 2015) while stations in italic were not. Note the unfortunate absence of EMEP stations providing information on sulfur species in 2014–15 in North-Western Europe. Red circles indicate the AERONET network stations of Dunkirk and SIRTA (Palaiseau).
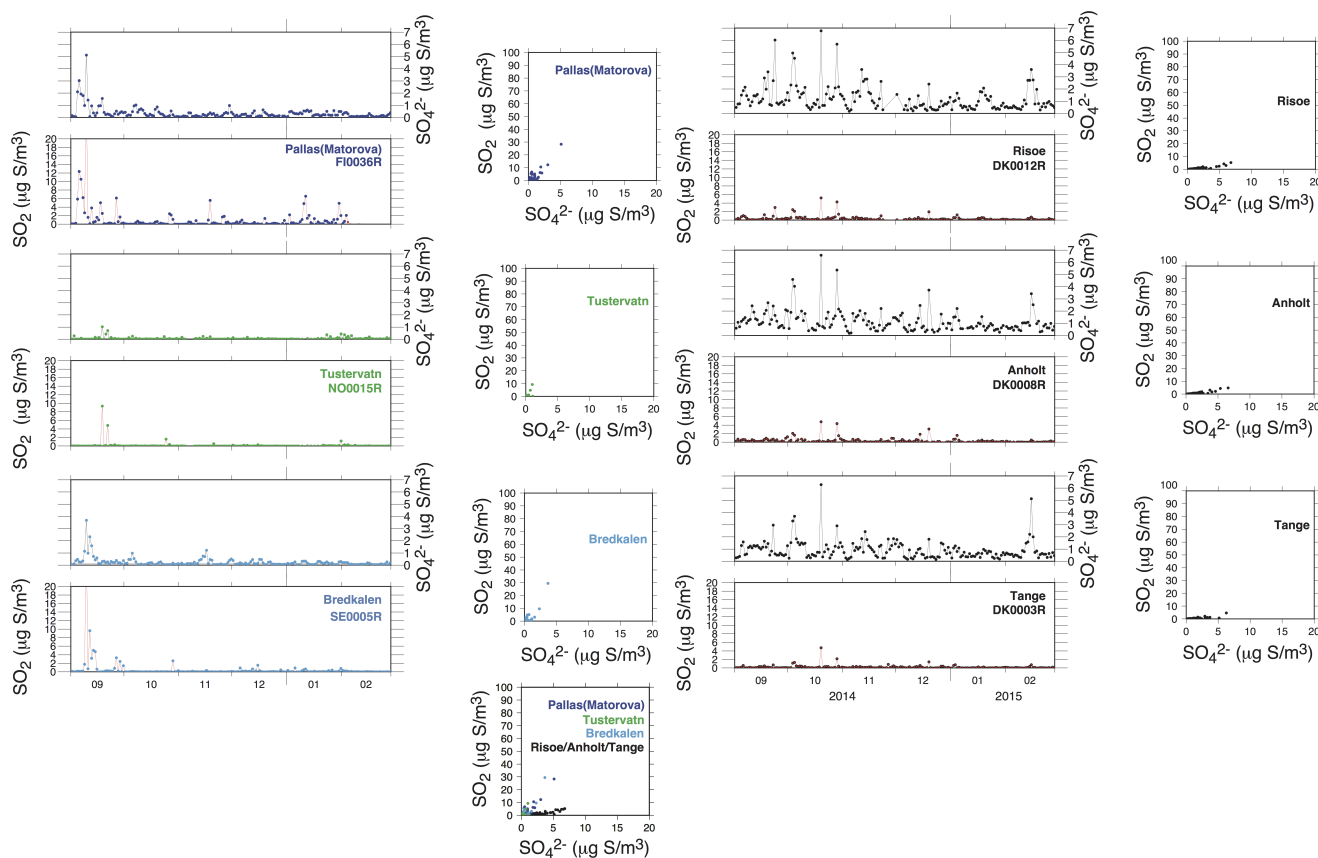
Figure 13. Time series (left) and scatter plots (right), covering the whole Holuhraun eruption of Bárðarbunga from Sept 2014 to Feb 2015, of SO_2 and SO_4^{2-} ground-level mass concentrations at various scandinavian EMEP stations impacted by the eruption.
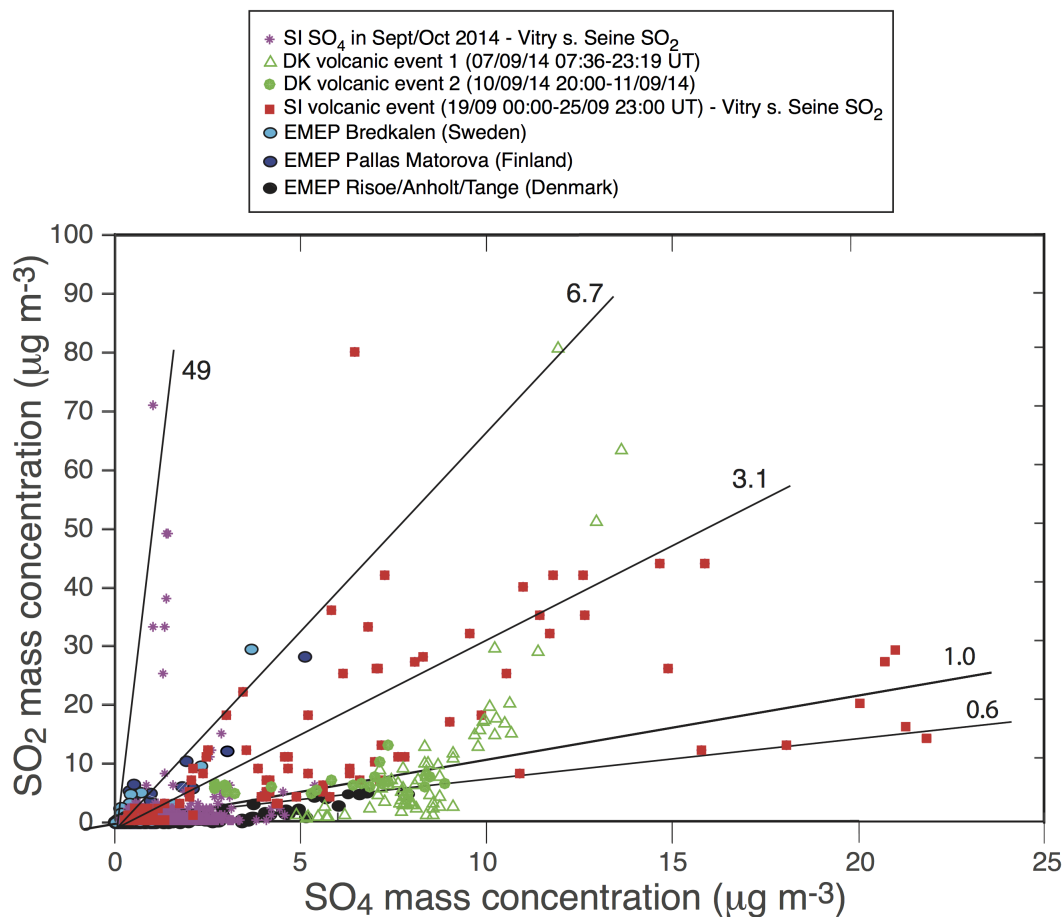
Figure 14. Scatter plot of SO_2 versus SO_4 mass concentrations recorded at scandinavian EMEP stations impacted by the Holuhraun eruption (blue and black ovals) and at ACSM (28% lower SO_4 RIE) and Atmo stations in France : three volcanic events of air pollution at Dunkirk/Port-East (in green) and at SIRTA (in red), background data at SIRTA (violet stars). Labels close to lines indicate the value of the slope, or in other words, the value of the SO_2:SO_4 mass concentration ratio along these lines.

Figure A1. Location in Dunkirk of the ACSM and Atmo stations at Port-East as well as the AERONET station. The aerial image used as base map is from the Geoportail of the French government (https://www.geoportail.gouv.fr). Note that the Arcelormittal site is the only one mentioned on the map as it represents the largest source of particles from steel industry in Dunkirk, well ahead of the other industrial activities, according to Clerc et al. (2012).
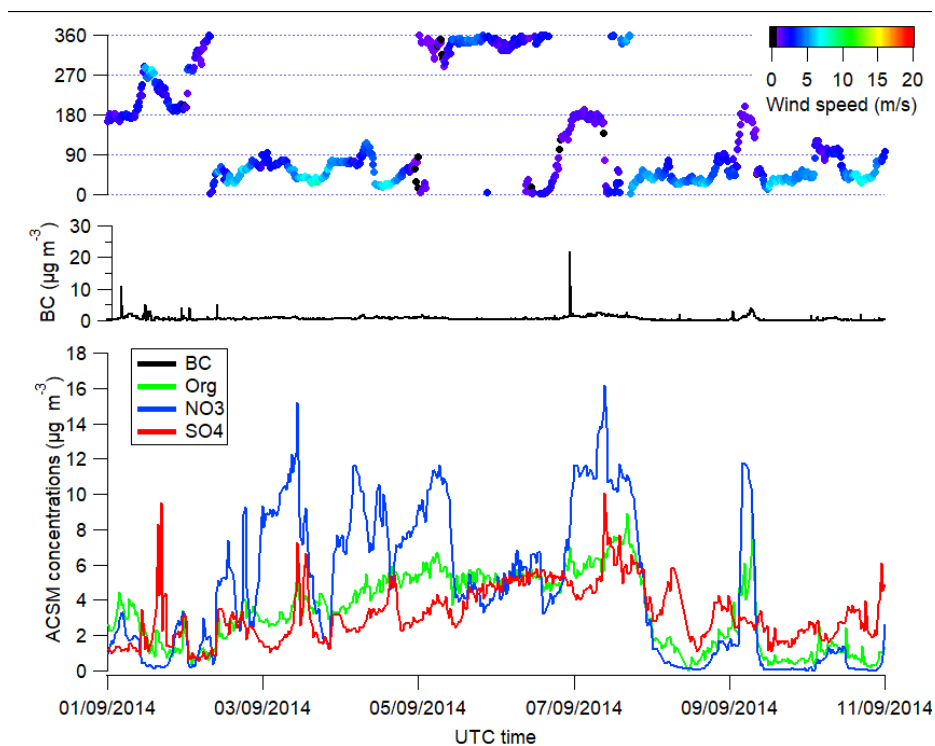
Figure A2. (Top) Local wind speed and direction, mass concentrations of (Middle) black carbon and (Bottom) ACSM sulfate, nitrate and organic aerosols in Dunkirk from 1 to 11 Sept 2014.